Hrd1 and ER-Associated Protein Degradation, ERAD, Are Critical Elements of the Adaptive ER Stress Response in Cardiac Myocytes

Shirin Doroudgar, Mirko Völkers, Donna J. Thuerauf, Mohsin Khan, Sadia Mohsin, Jonathan L. Respress, Wei Wang, Natalie Gude, Oliver J. Müller, Xander H.T. Wehrens, Mark A. Sussman, Christopher C. Glembotski

Rationale: **Hydroxymethyl glutaryl-coenzyme A reductase degradation protein 1 (Hrd1) is an endoplasmic reticulum (ER)-transmembrane E3 ubiquitin ligase that has been studied in yeast, where it contributes to ER protein quality control by ER-associated degradation (ERAD) of misfolded proteins that accumulate during ER stress. Neither Hrd1 nor ERAD has been studied in the heart, or in cardiac myocytes, where protein quality control is critical for proper heart function.**

Objective: **The objective of this study were to elucidate roles for Hrd1 in ER stress, ERAD, and viability in cultured cardiac myocytes and in the mouse heart, in vivo.**

Methods and Results: **The effects of small interfering RNA–mediated Hrd1 knockdown were examined in cultured neonatal rat ventricular myocytes. The effects of adeno-associated virus–mediated Hrd1 knockdown and overexpression were examined in the hearts of mice subjected to pressure overload–induced pathological cardiac hypertrophy, which challenges protein-folding capacity. In cardiac myocytes, the ER stressors, thapsigargin and tunicamycin increased ERAD, as well as adaptive ER stress proteins, and minimally affected cell death. However, when Hrd1 was knocked down, thapsigargin and tunicamycin dramatically decreased ERAD, while increasing maladaptive ER stress proteins and cell death. In vivo, Hrd1 knockdown exacerbated cardiac dysfunction and increased apoptosis and cardiac hypertrophy, whereas Hrd1 overexpression preserved cardiac function and decreased apoptosis and attenuated cardiac hypertrophy in the hearts of mice subjected to pressure overload.**

Conclusions: **Hrd1 and ERAD are essential components of the adaptive ER stress response in cardiac myocytes. Hrd1 contributes to preserving heart structure and function in a mouse model of pathological cardiac hypertrophy. (*Circ Res*. 2015;117:536-546. DOI: 10.1161/CIRCRESAHA.115.306993.)**

Key Words: endoplasmic reticulum stress ■ hydroxymethylglutaryl CoA reductases ■ myocytes, cardiac ■ protein folding ■ proteolysis

Cellular function depends on protein homeostasis, also known as proteostasis.[1] Proteostasis requires the efficient folding of newly synthesized proteins, as well as protein quality control and degradation, which decrease the accumulation of misfolded, potentially toxic proteins.[1] At least one-third of all proteins, including calcium handling proteins, transmembrane receptors, growth factors, and hormones, are synthesized, modified, and folded in the endoplasmic reticulum (ER), then trafficked to various membrane compartments, or secreted.[2] Thus, the environment in the ER must be optimal for efficient synthesis and folding of these important proteins.[3–5]

A variety of diseases, including many that affect the heart, challenge ER protein folding capacity.[6–9] Such challenges can be because of mutations in ER proteins, which can affect their folding or targeting, or to disease-related perturbations of the ER environment,[10] which lead to imbalanced proteostasis, and, in extreme cases, ER stress. ER stress contributes to pathology by impeding the production of critical ER proteins and by increasing the accumulation of potentially toxic misfolded proteins.

Editorial, see p 484

Original received June 9, 2015; revision received June 26, 2015; accepted July 1, 2015. In May 2015, the average time from submission to first decision for all original research papers submitted to *Circulation Research* was 15.49 days.

From the San Diego State University Heart Institute and the Department of Biology, San Diego State University, CA (S.D., M.V., D.J.T., M.K., S.M., N.G., M.A.S., C.C.G.); Department of Cardiology, University of Heidelberg, Heidelberg, Germany (M.V.); DZKH (German Centre for Cardiovascular Research) Partner Site Heidelberg/Mannheim, Heidelberg, Germany (M.V.); Department of Internal Medicine III (O.J.M.), University of Heidelberg, Heidelberg, Germany; Center for Translational Medicine, Temple University School of Medicine, Philadelphia, PA (M.K., S.M.); and Department of Molecular Physiology and Biophysics, Baylor College of Medicine, Houston, TX (J.L.R., W.W., X.H.T.W.).

The online-only Data Supplement is available with this article at http://circres.ahajournals.org/lookup/suppl/doi:10.1161/CIRCRESAHA.115.306993/-/DC1.

Correspondence to Christopher C. Glembotski, PhD, The SDSU Heart Institute and the Department of Biology, San Diego State University, 5500 Campanile Dr, San Diego, CA 92182. E-mail cglembotski@mail.sdsu.edu

Nonstandard Abbreviations and Acronyms

AAV	adeno-associated virus
ATF6	activating transcription factor 6α
ER	endoplasmic reticulum
ERAD	ER-associated degradation
HA	hemaglutinin
Hrd1	HMG-CoA reductase degradation protein 1
LV	left ventricle
SR	sarcoplasmic reticulum
TAC	transaortic constriction
TCR-α	T-cell antigen receptor α-chain
UPR	unfolded protein response

ER protein misfolding activates the unfolded protein response (UPR), a conserved signaling system that initiates multiple processes to restore proteostasis, including optimization of ER chaperone-assisted protein folding and increased misfolded protein degradation by ER-associated degradation (ERAD).[11] ERAD is a 4-step quality control process for removing terminally misfolded proteins from the ER by the cytosolic ubiquitin-proteasome system.[10,12,13] ER-transmembrane and luminal proteins that misfold during ER stress and fail quality control (Figure 1A, step 1) are transported out of the ER into the cytosol (step 2), where they are ubiquitylated on the cytosolic side of the ER by ER-transmembrane E3 ubiquitin ligases (step 3), which targets them for degradation by cytosolic proteasomes (step 4). Accordingly, ERAD is an adaptive process.[13] If ERAD and other aspects of the UPR fail to resolve ER stress, maladaptive features of the UPR, sometimes called maladaptive ER stress, guide cells toward apoptosis, which contributes to the tissue damage and organ dysfunction that are characteristic of pathologies associated with imbalanced proteostasis.[14,15]

UPR genes are regulated by several transcription factors including activating transcription factor 6α (ATF6), an ER-transmembrane protein.[16,17] Although not well studied in cardiac myocytes, or in the heart, in other cultured cell models ER protein misfolding triggers the translocation of ATF6 to the nucleus, where it induces certain ER stress response genes.[17] Although the causes and consequences of ER stress in the heart remain to be elucidated, previous studies have suggested that ATF6 regulates mainly adaptive ER stress responses.[18,19] Thus, identifying ATF6-regulated genes is required to understand mechanisms that maintain proteostasis and defend against the maladaptive ER stress response and potential cardiac dysfunction.

Our previous transcriptome analysis showed that in the mouse heart ATF6 induces genes that encode numerous ER-resident proteins predicted to contribute to enhancing ER protein folding through the adaptive ER stress response, including components of the ERAD machinery.[20] One of the genes induced by ATF6 in the heart is the ER-transmembrane E3 ubiquitin ligase, hydroxymethyl glutaryl-coenzyme A reductase degradation protein 1 (Hrd1; Figure 1A). Hrd1 was discovered in yeast and named for its ability to ubiquitylate the ER-transmembrane protein, hydroxymethyl glutaryl-coenzyme A reductase.[21] Since then, Hrd1 has been shown in yeast,[22,23] as well as in several mammalian cell lines,[24,25] to play a key role in ERAD-mediated degradation of a wide spectrum of misfolded proteins. Moreover, Hrd1 has been implicated as being beneficial in several neurodegenerative diseases,[26] and maladaptive in other diseases, such as liver cirrhosis[27] and rheumatoid arthritis.[28] In addition to Hrd1, other ER-transmembrane E3 ubiquitin ligases, such as E3 ubiquitin-protein ligase AMFR, E3 ubiquitin-protein ligase MARCH6, and E3 ubiquitin-protein ligase RNF139, also contribute to ERAD, although the range of substrates for these enzymes is more limited than Hrd1.[10] Remarkably, among ≈1000 E3 ubiquitin ligases in the genome,[29] Hrd1 was the only ER-transmembrane E3 ubiquitin ligase that was induced by ATF6 in the heart.[20] Because ER-transmembrane E3 ubiquitin ligases have not been examined in the cardiac context, we undertook the current study to investigate roles for Hrd1 in cultured cardiac myocytes and in the heart.

Methods

Further details on the Methods can be found in the Online Data Supplement.

Laboratory Animals

The research reported in this article has been reviewed and approved by the San Diego State University Institutional Animal Care and Use Committee and it conforms to the Guide for the Care and Use of Laboratory Animals published by the National Research Council.

Hrd1 Ubiquitylation Assay

The ubiquitin ligase activity of the Hrd1 used in this study was demonstrated as described in the Online Data Supplement.

ERAD Assay

ER-associated protein degradation (ERAD) was measured using a C terminally hemaglutinin (HA)-tagged version of the model substrate, T-cell antigen receptor α-chain (TCR-α), essentially as described,[30] but using adenovirus (AdV)-TCR-α-HA.

Statistics

Unless otherwise stated, values shown are mean±SEM and statistical treatments are 1-way ANOVA followed by Newman–Keuls post hoc analysis.

Results

Hrd1 Is Induced by ATF6, X-Box-Binding Protein 1, and ER Stress in Cardiac Myocytes

To examine Hrd1 gene expression in response to ER stress in cardiac myocytes, we determined the effects of ATF6 and another ER stress-inducible transcription factor, X-box-binding protein 1, on Hrd1 expression in cultured neonatal rat ventricular myocytes. Hrd1 mRNA increased when cardiac myocytes were infected with AdV encoding activated ATF6, or activated X-box-binding protein 1 (Figure 1B). Hrd1 mRNA also increased when cardiac myocytes were treated with chemical inducers of ER stress, tunicamycin, thapsigargin, or dithiothreitol (Figure 1C), which cause ER protein misfolding by inhibiting protein glycosylation,[31] decreasing ER calcium,[32] or altering ER redox status,[33] respectively.

To detect Hrd1 protein, we generated a rabbit antiserum to the C-terminal cytosolic domain of human Hrd1, which is conserved in mouse and rat Hrd1. Using this antiserum, we showed that Hrd1 protein increased when cultured cardiac myocytes were infected with AdV encoding activated ATF6 or activated X-box-binding protein 1 (Figure 1D and 1E), or

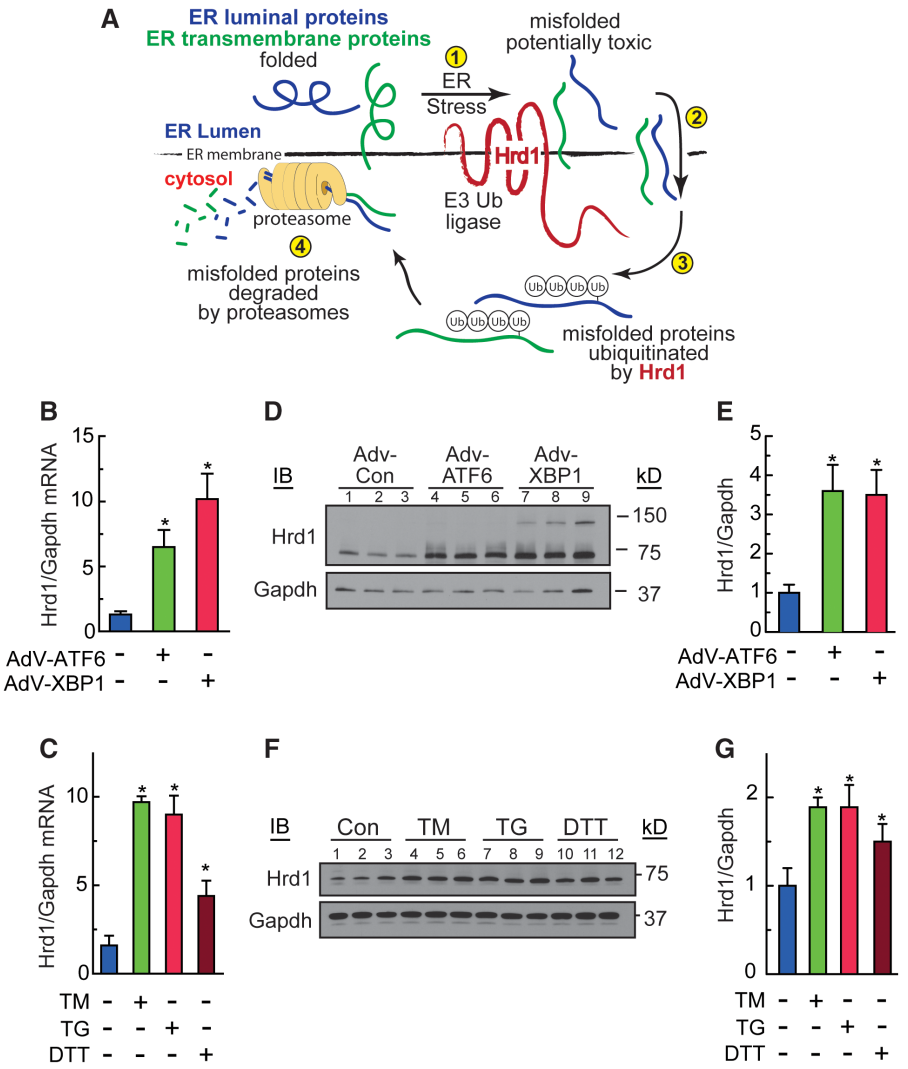

Figure 1. Characterization of Hrd1 expression in cardiac myocytes. A, Diagram of endoplasmic reticulum (ER)–associated protein degradation. **B**, **D**, and **E**, Cultured cardiac myocytes were treated with adenovirus AdV-Con (control), AdV-activating transcription factor 6α (ATF6), or AdV-X-box-binding protein 1 (XBP1) for 48 hours. Hrd1 and Gapdh mRNA B, or protein D, were measured by quantitative reverse transcriptase polymerase chain reaction (qRT-PCR) or immunoblotting, respectively. IB, antibodies used for immunoblotting. **E**, Densitometry of the immunoblot shown in **D**. **C**, **F**, and **G,** Cultured cardiac myocytes were treated with tunicamycin (TM) 10 μg/mL, thapsigargin (TG) 1 μmol/L, or dithiothreitol (DTT) 1 mmol/L for 20 hours. Hrd1 and Gapdh mRNA C, or protein F, were measured by qRT-PCR or immunoblotting, respectively. **G**, Densitometry of the immunoblot shown in **F**. **P*≤0.05 different from control. Ub indicates ubiquitin.

when they were treated with tunicamycin, thapsigargin, or dithiothreitol (Figure 1F and 1G). Thus, Hrd1 was upregulated in cultured cardiac myocytes by ER stress and by key transcription factors of the UPR gene program.

Hrd1 Knockdown Augments ER Stress Gene Expression and Decreases Cardiac Myocyte Viability

To examine the function of endogenous Hrd1, we used an small interfering RNA targeted to Hrd1, (siHrd1), which decreased Hrd1 in cultured cardiac myocytes by as much as 75% (Figure 2A and 2B). Hrd1 knockdown increased the ER stress markers, Grp94 and Grp78 in untreated cells, as well as in cells treated with tunicamycin or thapsigargin for 48 hours (Figure 2A, 2C, and 2D) or 72 hours (Online Figure IA, IC, and ID). These results indicated that a reduction in Hrd1 increased misfolded ER proteins and subsequent ER stress. However, most dramatic was the increase in the ER stress–inducible protein, C/EBP-homologous protein, in cells treated with tunicamycin or thapsigargin (Figure 2A and 2E; Online Figure IA and IE). C/EBP-homologous protein is often associated with maladaptive ER stress and cell death. Accordingly, the effects of Hrd1 knockdown on cardiac myocyte viability were examined. Hrd1 knockdown decreased cardiac myocyte viability in cells treated with tunicamycin or thapsigargin (Figure 2F and 2G; Online Figure IF and IG). Moreover, ER stress–mediated activation of caspase-12, a marker of maladaptive ER stress and inducer of apoptosis, was also increased by Hrd1 knockdown in cells treated with tunicamycin or thapsigargin (Figure 2H and 2I). In addition, Hrd1 knockdown decreased cell number significantly in neonatal rat ventricular myocytes subjected to simulated ischemia/reperfusion (Figure 2J). Hrd1 knockdown was also shown to decrease protein ubiquitylation (Online Figure IH). These results indicate that endogenous Hrd1 protects cardiac

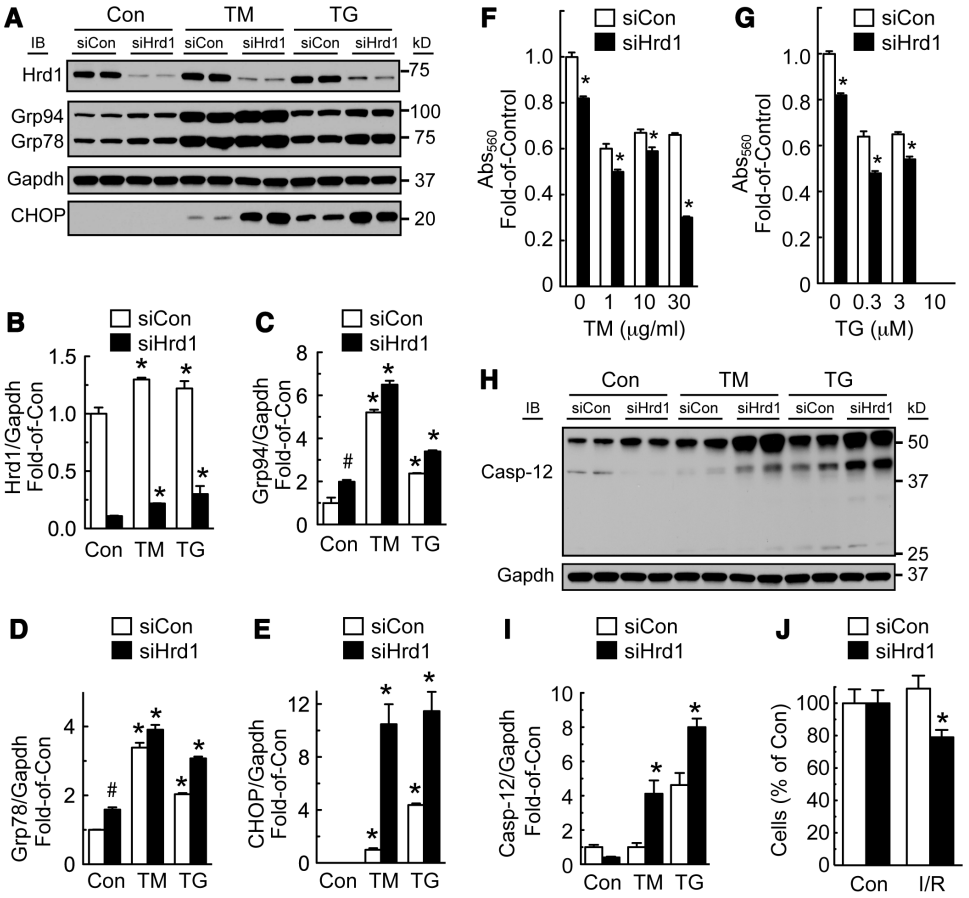

Figure 2. Effects of Hrd1 knockdown on ER stress and myocyte viability. Cultured cardiac myocytes were treated with siCon (control small interfering RNA) or siHrd1 (Hrd1 small interfering RNA) for 48 hours, and then vehicle, tunicamycin (TM; 10 μg/mL) or thapsigargin (TG; 1 μmol/L) for 48 hours. **A**, Hrd1, Grp94, Grp78, Gapdh, and C/EBP-homologous protein (CHOP) were measured by immunoblotting. IB, antibodies used for immunoblotting. **B** to **E**, Densitometry of the blots shown in **A** normalized to vehicle-treated siCon, except for CHOP, which was normalized to TM-treated siCon. **P*≤0.05 different from Con. #*P*≤0.05 different from Con/siCon. **F** and **G**, Cultured cardiac myocytes were treated with siCon or siHrd1 for 48 hours, and then with various doses of TM or TG for 48 hours, after which cell viability was determined by MTT (3-(4,5-dimethylthiazol-2-yl)-2,5-diphenyltetrazolium bromide) assay. **P*≤0.05 different from siCon at the same dose and time of TM or TG treatment. Note: at 10 μmol/L TG there was no MTT value in either siCon or siHrd1. **H**, Cultured cardiac myocytes were treated with siCon or siHrd1 and then with vehicle, TM, or TG for 48 hours. Extracts were then immunoblotted for caspase-12. **I**, Densitometry of the 40 kDa active version of caspase-12, normalized to vehicle-treated siCon cells. **P*≤0.05 different from treatment-matched siCon. **J**, Cultured cardiac myocytes were treated with siCon or siHrd1, and then subjected to simulated ischemia/reperfusion (I/R), after which cell numbers were determined by microscopy. **P*≤0.05 different from Con/siHrd1, as determined by *t* test.

myocytes against cell death caused by the maladaptive ER stress response.

Effect of Hrd1 Knockdown on ERAD

Because Hrd1 is best known for its roles in ERAD, but functional roles for ERAD have not been investigated in cardiac myocytes, we examined the effects of Hrd1 knockdown on ERAD in cardiac myocytes using an HA epitope-tagged version of the TCR-α-HA as a model misfolded ER protein.[30] When expressed in cells that do not normally express the other TCR subunits, TCR-α-HA, an ER-transmembrane protein, misfolds and is degraded by ERAD.[30,34] Accordingly, cultured cardiac myocytes that had been subjected to Hrd1 knockdown were infected with an AdV that expresses TCR-α-HA. The rate of TCR-α degradation, which is a measure of ERAD, was then assessed by examining TCR-α-HA levels by anti-HA immunoblotting after various times of blocking protein synthesis with cycloheximide. In control cells (siCon), tunicamycin and thapsigargin increased the rate of ERAD, as evidenced by a decrease in TCR-α-HA levels after each time of cycloheximide treatment (Figure 3A, siCon; Figure 3B and 3D). This finding suggests that ER stress–mediated upregulation of proteins that comprise the ERAD machinery augments the degradation of misfolded ER proteins. In contrast, when Hrd1 was knocked down, tunicamycin and thapsigargin dramatically decreased ERAD (Figure 3A, siHrd1; Figure 3C and 3E). Moreover, the rate of ERAD was decreased by Hrd1 knockdown even in the absence of ER stress. These results demonstrate that endogenous Hrd1 plays a key role in the adaptation of cardiac myocytes to ER protein misfolding.

Hrd1 Knockdown Is Maladaptive in a Mouse Model of Pathological Cardiac Hypertrophy

To determine roles for endogenous Hrd1 during cardiac pathology, mice were injected with 10^{11} genome-containing units of adeno-associated virus 9 encoding either a control small hairpin RNA (AAV9-sh-Con) or a small hairpin

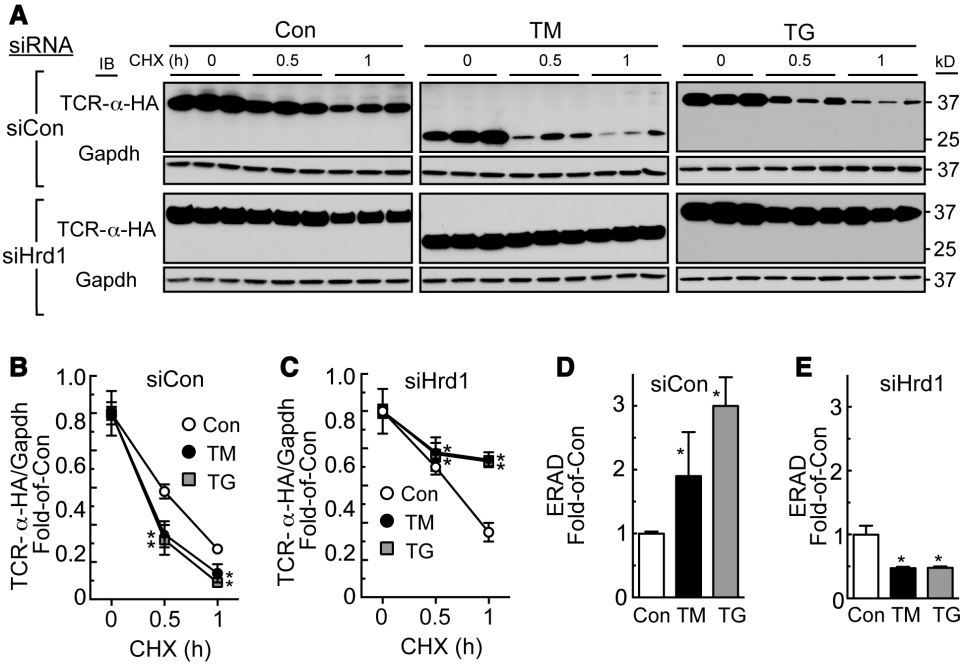

Figure 3. Effects of Hrd1 knockdown, tunicamycin (TM), and thapsigargin (TG) on ERAD. A, Cultured cardiac myocytes were treated with adenovirus (AdV)-T-cell antigen receptor α-chain (TCR)-α-hemaglutinin (HA) and siCon (control small interfering RNA) or siHrd1 (Hrd1 small interfering RNA) for 48 hours, and then with vehicle, TM (10 μg/mL) or TG (1 μmol/L) for 24 hours. Cultures were then treated with cycloheximide (CHX) for the times shown (hours), and then immunoblotted for TCR-α-HA and Gapdh. IB, antibodies used for immunoblotting. The mass of TCR-α-HA decreased on TM treatment because TM inhibits its glycosylation. **B** and **C**, Densitometry of the TCR-α-HA blots shown in **A**. **P*≤0.05 different from Con at the same CHX treatment time. **D** and **E**, ERAD is displayed here as the relative rates of TCR-α-HA degradation at the 1-hour CHX treatment time. **P*≤0.05 different from Con.

RNA targeted to Hrd1 (AAV9-sh-Hrd1), and then subjected to sham or transaortic constriction (TAC) surgery to produce pressure overload–induced pathological cardiac hypertrophy (Figure 4A). Because of its effects on increasing cardiac myocyte protein synthesis, pathological cardiac hypertrophy can potentially challenge cellular protein folding and quality control machinery. Immunoblots of the mouse hearts showed that AAV9-sh-Hrd1 decreased Hrd1 levels of sham and TAC mouse hearts by ≈50% (Figure 4B). Echocardiography showed that, when compared with control, Hrd1 knockdown did not significantly affect fractional shortening (Figure 4C, blue versus green) or ejection fraction (Online Table I). However, in mice subjected to TAC surgery, Hrd1 knockdown exacerbated the functional impairment, as evidenced by further significant decreases in fractional shortening (Figure 4C, red versus brown) and ejection fraction (Online Table I).

In terms of left ventricular (LV) structure, in mice subjected to TAC, Hrd1 knockdown increased LV end diastolic and systolic volumes (Figure 4D and 4E), as well as LV diastolic and systolic inner diameters (Online Table I), all of which are indicators of pathological LV dilation in response to pressure overload. These results indicated that Hrd1 knockdown accelerated disease progression in response to pressure overload, as evidenced by worsened systolic dysfunction, as well as increased systolic and diastolic LV dilation.

In terms of cardiac hypertrophy, when compared with control, Hrd1 knockdown increased heart weights in mice subjected to sham surgery (Figure 4F, blue versus green), suggesting that endogenous Hrd1 is a regulator of cardiac growth and knocking down Hrd1 may prime the heart for a hypertrophic growth response. This trend was also seen when LV mass was calculated from the echocardiography data, although it did not reach statistical significance (Online Table I). In control mice, heart weights were increased by TAC (Figure 4F, red), consistent with the expected pressure overload–induced cardiac hypertrophy. Hrd1 knockdown resulted in a further increase in heart weight by TAC (Figure 4F, brown) but, as determined gravimetrically, this increase did not reach significance. However, when calculated from the echocardiography data, the increase in LV mass in mice subjected to TAC was significantly increased by Hrd1 knockdown, when compared with control (Online Table I).

With regards to genetic markers of hypertrophy, Hrd1 knockdown increased the levels of atrial natriuretic factor, B-type natriuretic peptide, and β-myosin heavy chain in the hearts of mice subjected to TAC (Figure 4G, group 3 versus 4), consistent with exacerbated hypertrophy by Hrd1 knockdown. The level of collagen 1A1 was also increased by Hrd1 knockdown (Figure 4G), suggesting an increase in fibrosis, which was supported by histological examination (Figure 5A–5D). Finally, examination of apoptosis in mouse heart sections using a terminal deoxynucleotidyl transferase dUTP nick end labeling stain also showed that Hrd1 knockdown increased the number of terminal deoxynucleotidyl transferase dUTP nick end labeling positive nuclei (Figure 5E). Thus, by most measures, Hrd1 knockdown exacerbated cardiac pathology in the hearts of mice subjected to pressure overload.

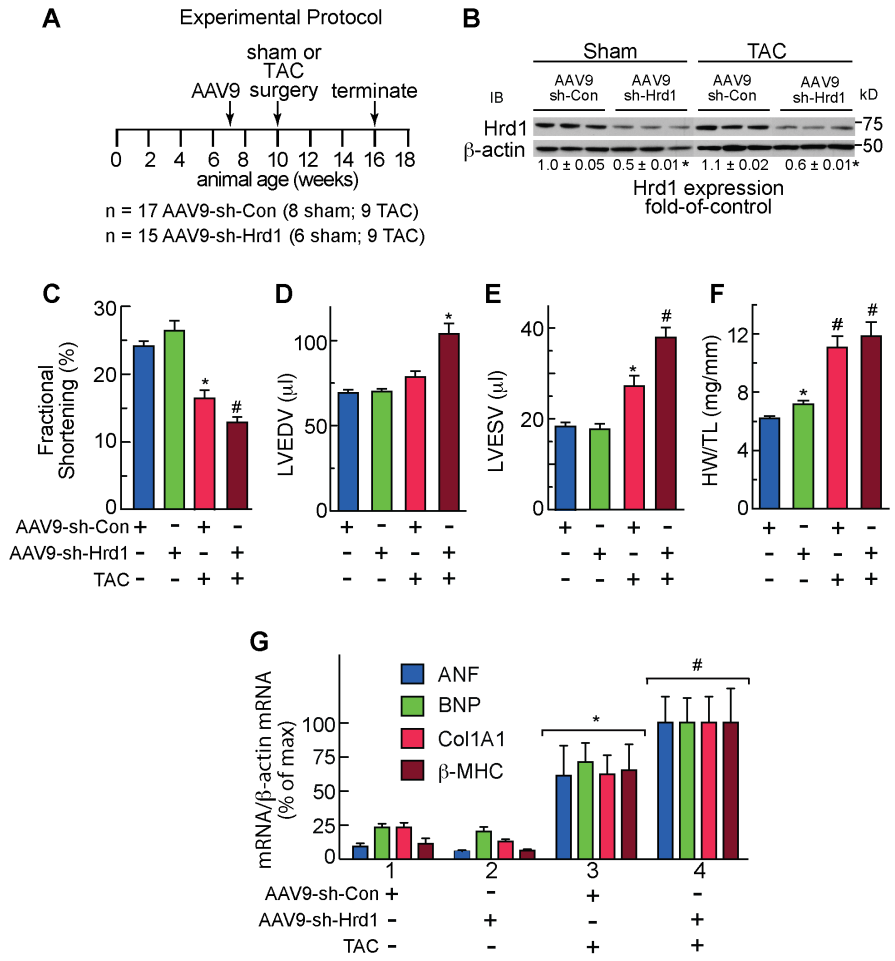

Figure 4. Hrd1 knockdown impairs cardiac function. A, Experimental protocol for adeno-associated virus (AAV) 9 administration, transaortic constriction (TAC), and termination of the experiment. n indicates number of mice used for each treatment. **B**, Immunoblots of AAV9-sh-Con (AAV9-encoded control small hairpin RNA) or AAV9-sh-Hrd1 (AAV9-encoded Hrd1 small hairpin RNA) mouse heart extracts. **C** to **E,** Echocardiography of AAV9-sh-Con and AAV9-sh-Hrd1–treated mice subjected to sham or TAC surgery. Echocardiography was done just before euthanization of the animal. **C**, Fractional shortening (%). **D** and **E**, LVEDV and LVESV, respectively. **F**, Heart weights normalized to tibia lengths (HW/TL). **G**, mRNA levels in mouse heart extracts were determined by quantitative reverse transcriptase polymerase chain reaction. *,#$P \leq 0.05$ different from all other values. Additional echocardiography data and statistical analyses can be found in Online Table I. β-MHC indicates β-myosin heavy chain; ANF, atrial natriuretic factor; BNP, B-type natriuretic peptide; Col1A1, collagen 1A1; LVEDV, left ventricular end-diastolic volume; and LVESV, left ventricular end-systolic volume.

Hrd1 Overexpression Is Adaptive in a Mouse Model of Pathological Cardiac Hypertrophy

Because Hrd1 loss-of-function was maladaptive, we examined whether Hrd1 gain-of-function would be adaptive in the mouse heart. Accordingly, we generated a recombinant AAV9 encoding an untagged version of mouse Hrd1. Expression of Hrd1 was directed to ventricular myocytes using a previously described form of the myosin regulatory light chain 2 promoter,[35,36] which we previously showed to support increased protein expression in >80% of mouse cardiac myocytes, in vivo.[37,38] In the present study, 10^{11} genome-containing units of AAV9-Con or AAV9-Hrd1 were administered to mice by tail vein injection. Immunocytofluorescence showed that, when compared with AAV9-Con, AAV9-Hrd1 increased Hrd1 expression in most cardiac myocytes in mouse hearts, and that some myocytes expressed more Hrd1 than others (Online Figure IIA and IIB). Additional immunocytofluorescence showed that Hrd1 colocalized with cardiac troponin T and, to some extent, with sarcoplasmic/endoplasmic reticulum calcium ATPase 2a (Online Figure IIC and IID), consistent with Hrd1 localization to the longitudinal sarcoplasmic reticulum (SR). Because Hrd1 seemed to localize to the SR, the effects of Hrd1 overexpression on Ca^{2+} transients in adult mouse cardiac myocytes were examined. Overexpression of Hrd1 did not change the Ca^{2+} transient amplitude, the rate of Ca^{2+} removal from the cytosol by sarcoplasmic/endoplasmic reticulum calcium ATPase 2, SR Ca^{2+} concentration, or sarcolemmal sodium–calcium exchanger activity (Online Figure IIIA–IIID). Moreover, Hrd1 overexpression did not affect Ca^{2+} spark properties (Online Figure IIIE–IIIH). Therefore, Hrd1 overexpression had no adverse effects on contractile Ca^{2+} handling in the heart.

To examine the effects of Hrd1 overexpression on cardiac pathology, mice that had been injected with either AAV9-Con or AAV9-Hrd1 were subjected to sham or TAC

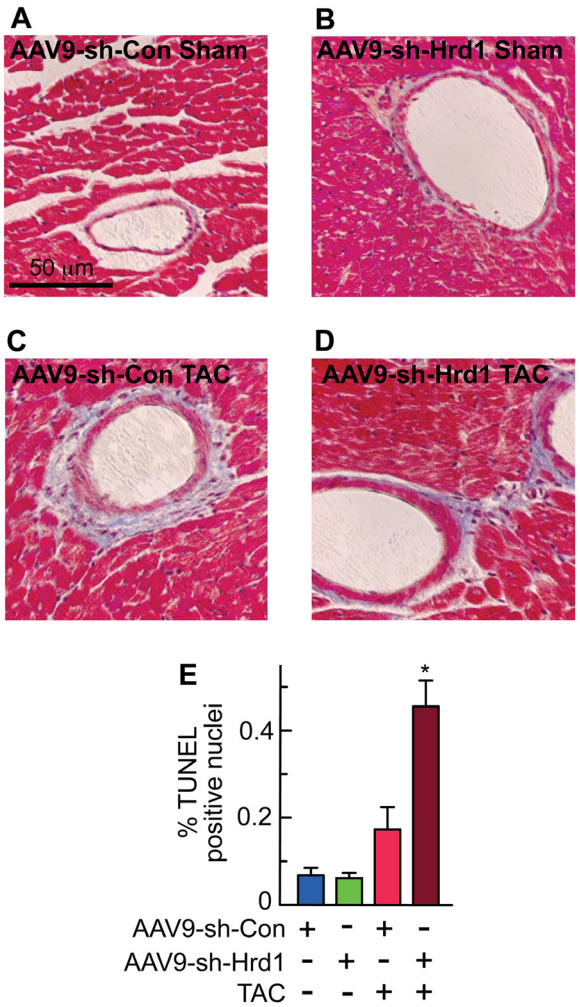

Figure 5. Histology and terminal deoxynucleotidyl transferase dUTP nick end labeling (TUNEL) analyses of mouse hearts treated with adeno-associated virus (AAV)-sh-Con and AAV9-sh-Hrd1. A to **D,** Sections of hearts from mice treated with either AAV9-sh-Con (AAV9-encoded control small hairpin RNA) or AAV9-sh-Hrd1 (AAV9-encoded Hrd1 small hairpin RNA), and then subjected to sham or transaortic constriction (TAC) surgery, as described in the Experimental Protocol shown in Figure 4A, were stained with Masson's trichrome to examine fibrosis (blue). **E**, Sections of hearts from mice treated with either AAV9-sh-Con or AAV9-sh-Hrd1, and then subjected to TAC were analyzed for apoptosis by TUNEL staining, and then quantified to determine % of nuclei that were TUNEL-positive. *$P \leq 0.05$ different from all other values.

surgery (Figure 6A). Immunoblots showed that AAV9-Hrd1 increased Hrd1 expression in both sham and TAC-treated mouse hearts (Figure 6B). TAC resulted in a slight increase in Hrd1 protein (Figure 6B), as well as Hrd1 mRNA (Online Figure IVA). Echocardiography showed that Hrd1 overexpression did not affect fractional shortening (Figure 6C, blue versus green) or ejection fraction (Online Table II) in mice subjected to sham surgery. However, Hrd1 overexpression improved fractional shortening and ejection fraction in mice subjected to TAC (Figure 6C, red versus brown; Online Table II). In terms of LV structure, Hrd1 overexpression also diminished TAC-mediated increases left ventricular end-diastolic volume and left ventricular end-systolic volume (Figure 6D and 6E, red versus brown), as well as LV diameter (Online Table II). In terms of cardiac hypertrophy, AAV9-Con–treated mice subjected to TAC exhibited increased heart weights, which were diminished in AAV9-Hrd1–treated mice (Figure 6F, red versus brown). Hrd1 overexpression decreased the levels of atrial natriuretic factor, B-type natriuretic peptide, and β-myosin heavy chain in mice subjected to TAC (Figure 6G, group 3 versus 4). Moreover, the level of collagen 1A1 in mice subjected to TAC was also decreased by Hrd1 overexpression (Figure 6G), suggesting a decrease in fibrosis, which was supported by histological examination (Figure 7A–7D). Finally, examination of apoptosis in mouse heart sections using a terminal deoxynucleotidyl transferase dUTP nick end labeling stain also showed that Hrd1 overexpression decreased the number of terminal deoxynucleotidyl transferase dUTP nick end labeling positive nuclei (Figure 7E). Thus, by most measures, Hrd1 overexpression decreased cardiac pathology in the hearts of mice subjected to pressure overload.

To examine the effects of Hrd1 overexpression on cardiac myocyte growth directly, we generated an AdV encoding Hrd1, which resulted in overexpression of Hrd1 in cultured cardiac myocytes by ≈3-fold over control (Online Figure VA). Immunocytofluorescence showed that, when compared with AdV-Con, AdV encoding Hrd1 increased the levels of Hrd1, which colocalized with ER proteins (Online Figure VI). Overexpression of Hrd1 decreased myocyte surface area and protein synthesis, as well as expression of atrial natriuretic factor and B-type natriuretic peptide, 2 markers of hypertrophic cardiac myocyte growth (Online Figure VB–VE). These results are consistent with the ability of Hrd1 to diminish hypertrophy, in vivo and indicate that Hrd1 exhibits cardiac myocyte growth moderating effects.

Discussion

ER Stress and Heart Disease

Many diseases, including heart disease, are associated with protein misfolding, which contributes to organ dysfunction.[2,39–42] Such protein misfolding can take place in the ER, as well as elsewhere in cardiac myocytes. Protein quality control outside the ER in cardiac myocytes has been addressed in several relatively recent studies[42]; however, less is known about the effects of protein misfolding in the ER of cardiac myocytes. Although protein misfolding can have dire consequences, regardless of where it takes place, disease-related ER protein misfolding is particularly problematic in cardiac myocytes, because it could affect the levels of key secreted and membrane proteins, such as calcium-handling proteins and adrenergic receptors, which can impair cardiac myocyte function. Moreover, some forms of cardiac disease, such as those associated with hypertrophy, can increase protein synthesis, which potentially challenges an already disease-impaired ER protein-folding environment.[19,39,43] Although not studied extensively in cardiac myocytes, in other model cell types, ER protein misfolding activates the UPR, which is designed to restore ER protein folding and degrade misfolded proteins, which are processes that are essential for the adaptive ER stress response. Therefore, throughout essentially all of a cellular lifetime, ER stress is met with adaptive responses.[11]

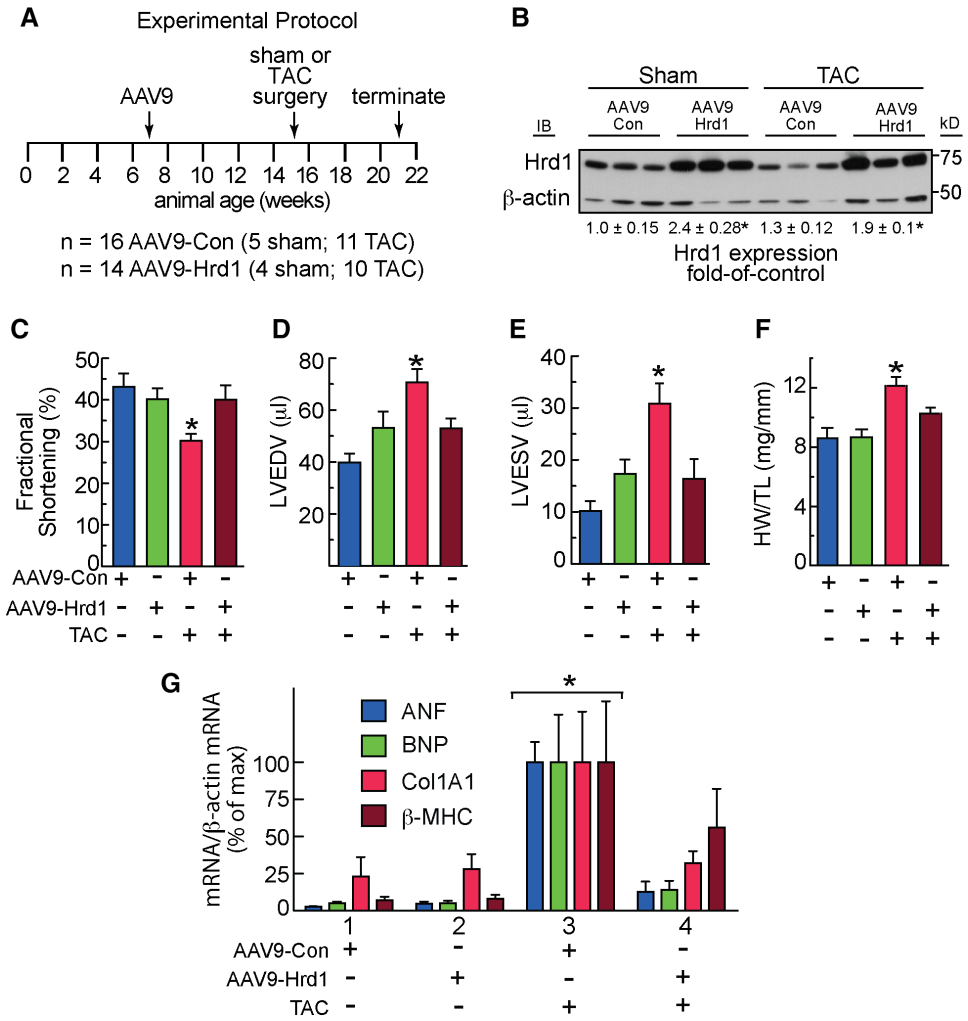

Figure 6. Hrd1 overexpression preserves cardiac function. A, Experimental protocol for adeno-associated virus (AAV) 9 administration, transaortic constriction (TAC), and termination of the experiment. n indicates number of mice used for each treatment. **B**, Immunoblots of AAV9-Con or AAV9-Hrd1 mouse heart extracts. **C** to **E,** Echocardiography of AAV9-Con and AAV9-Hrd1–treated mice subjected to sham or TAC surgery. Echocardiography was done just before euthanization of the animal. **C**, Fractional shortening (%). **D** and **E**, LVEDV and LVESV, respectively. **F**, Heart weights normalized to tibia lengths (HW/TL). **G,** mRNA levels in mouse heart extracts were determined by quantitative reverse transcriptase polymerase chain reaction. *$P \leq 0.05$ different from all other values. Additional echocardiography data and statistical analyses can be found in Online Table II. β-MHC indicates β-myosin heavy chain; ANF, atrial natriuretic factor; BNP, B-type natriuretic peptide; Col1A1, collagen 1A1; LVEDV, left ventricular end-diastolic volume; and LVESV, left ventricular end-systolic volume.

However, when such adaptive responses are not sufficient to restore ER proteostasis, continued ER stress can impair cardiac myocyte function and, ultimately, it can lead to cell death and organ damage.[15]

The Adaptive ER Stress Response and Cardiac Development

In contrast to the neonatal heart, we found that the adult heart expresses low levels of Hrd1, as well as Grp78 and ATF6 (Online Figure IVB). Previous studies of a variety of tissues, including liver, kidney, brain, and heart, have shown that other proteins that are part of the ER protein synthesis and quality control machinery are also expressed at higher levels early in the development when compared with the adult.[44–46] Moreover, targeted deletion of the genes encoding several of these proteins, such as Grp78, Grp94, calreticulin, and Hrd1, is embryonic-lethal in mice, and in many of these cases, this lethality is associated with impaired cardiac development,[47–50] underscoring the essential nature of these genes in the embryonic heart. The relatively high levels of ER proteins in early development may be required to support cellular differentiation and the high rate of production of secreted and membrane proteins. Moreover, in the developing heart, cardiac myocytes proliferate and grow in size, placing demands on the ER protein synthesis and folding machinery. In addition, the SR must grow dramatically to meet the needs of the developing excitation–contraction coupling machinery in growing cardiac myocytes. This SR expansion requires active lipid synthesis in the ER, as well as synthesis, proper folding, and trafficking of the proteins that participate in contractile calcium handling. Therefore, although it is not surprising that levels of Hrd1, as well as other ER protein quality control proteins, are high in the developing heart it has been previously unappreciated that in the adult heart, the adaptive ER stress response may be

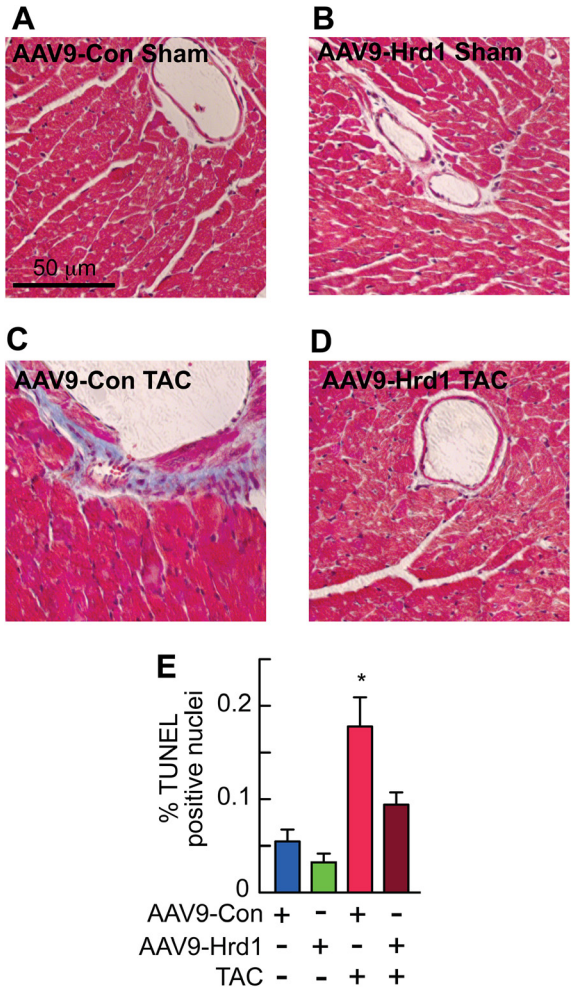

Figure 7. Histology and terminal deoxynucleotidyl transferase dUTP nick end labeling (TUNEL) analyses of mouse hearts treated with adeno-associated virus (AAV) 9-Con and AAV9-Hrd1. A to **D**, Sections of hearts from mice treated with either AAV9-Con or AAV9-Hrd1, and then subjected to sham or transaortic constriction (TAC) surgery, as described in the Experimental Protocol shown in Figure 6A, were stained with Masson's trichrome to examine fibrosis (blue). **E**, Sections of hearts from mice treated with either AAV9-Con or AAV9-Hrd1, and then subjected to TAC were analyzed for apoptosis by TUNEL staining, and then quantified to determine % of nuclei that were TUNEL-positive. *$P \leq 0.05$ different from all other values.

less dynamic and may therefore exhibit a narrower range of responsiveness to misfolded protein accumulation, than in the developing heart.

Conclusions

Previous studies have shown the importance of the transcription factors, ATF6 and X-box-binding protein 1, in the adaptive ER stress response in ischemic and hypertrophic heart disease in mice.[19,51–53] The present study demonstrates that a gene that can be induced by these transcription factors, Hrd1, contributes to the adaptive ER stress response in cultured cardiac myocytes and that it preserves cardiac function in a mouse model of pathological cardiac hypertrophy. Based on this study, we hypothesize that under certain conditions, sufficient levels of Hrd1 facilitate the degradation of misfolded proteins in the ER, which adaptively enhances myocyte viability. However, when Hrd1 is not sufficient, such as in the adult heart, pathology-driven maladaptive accumulation of misfolded proteins threatens myocyte viability and cardiac function. This is the first study to report on roles for any ER-transmembrane E3 ubiquitin ligase and ERAD in cardiac myocytes and in the mouse heart, in vivo. Moreover, this is the first study to show that ER stress accelerates ERAD in a Hrd1-dependend manner in cardiac myocytes.

Acknowledgments

We thank Dr Hajjar (Mount Sinai Hospital) for providing some of the plasmids that were used to generate adeno-associated virus 9, Dr Kopito (Stanford University) for the plasmid encoding an HA-tagged version of the T-cell antigen receptor α-chain.

Sources of Funding

S. Doroudgar was supported by grants from the Rees-Stealy Research Foundation, the SDSU Heart Institute, the San Diego Chapter of the Achievement Rewards for College Scientists Foundation, the American Heart Association (Predoctoral Fellowship 10PRE3410005), and the Inamori Foundation. M. Völkers was supported by the Deutsche Forschungsgemeinschaft 1659/1-1. J.L. Respress was supported by the National Institutes of Health (NIH) grant T32 HL007676-23. O.J. Müller was supported by the DZHK (German Centre for Cardiovascular Research) and by the BMBF (German Ministry of Education and Research). X.H.T. Wehrens was supported by the NIH grants R01 HL089598 and R01 HL091947, and American Heart Association Grant 13EIA14560061. M.A. Sussman was supported by the NIH grants R37 HL091102, R01 HL105759, R01 HL067245, R01 HL113656, R01 HL117163, R01 HL113647, and P01 HL 08577. C.C. Glembotski was supported by the NIH grants R01 HL75573, R01 HL104535, R03 EB011698, and P01 HL085577.

Disclosures

None.

References

1. Balch WE, Morimoto RI, Dillin A, Kelly JW. Adapting proteostasis for disease intervention. *Science*. 2008;319:916–919. doi: 10.1126/science.1141448.
2. Glembotski CC. Roles for the sarco-/endoplasmic reticulum in cardiac myocyte contraction, protein synthesis, and protein quality control. *Physiology (Bethesda)*. 2012;27:343–350. doi: 10.1152/physiol.00034.2012.
3. Gidalevitz T, Stevens F, Argon Y. Orchestration of secretory protein folding by ER chaperones. *Biochim Biophys Acta*. 2013;1833:2410–2424. doi: 10.1016/j.bbamcr.2013.03.007.
4. Amm I, Sommer T, Wolf DH. Protein quality control and elimination of protein waste: the role of the ubiquitin-proteasome system. *Biochim Biophys Acta*. 2014;1843:182–196. doi: 10.1016/j.bbamcr.2013.06.031.
5. Guerriero CJ, Brodsky JL. The delicate balance between secreted protein folding and endoplasmic reticulum-associated degradation in human physiology. *Physiol Rev*. 2012;92:537–576. doi: 10.1152/physrev.00027.2011.
6. Dickhout JG, Carlisle RE, Austin RC. Interrelationship between cardiac hypertrophy, heart failure, and chronic kidney disease: endoplasmic reticulum stress as a mediator of pathogenesis. *Circ Res*. 2011;108:629–642. doi: 10.1161/CIRCRESAHA.110.226803.
7. Minamino T, Komuro I, Kitakaze M. Endoplasmic reticulum stress as a therapeutic target in cardiovascular disease. *Circ Res*. 2010;107:1071–1082. doi: 10.1161/CIRCRESAHA.110.227819.
8. Doroudgar S, Glembotski CC. New concepts of endoplasmic reticulum function in the heart: programmed to conserve. *J Mol Cell Cardiol*. 2013;55:85–91. doi: 10.1016/j.yjmcc.2012.10.006.

9. Millott R, Dudek E, Michalak M. The endoplasmic reticulum in cardiovascular health and disease. *Can J Physiol Pharmacol*. 2012;90:1209–1217. doi: 10.1139/y2012-058.
10. Olzmann JA, Kopito RR, Christianson JC. The mammalian endoplasmic reticulum-associated degradation system. *Cold Spring Harb Perspect Biol*. 2013;5:. doi: 10.1101/cshperspect.a013185.
11. Walter P, Ron D. The unfolded protein response: from stress pathway to homeostatic regulation. *Science*. 2011;334:1081–1086. doi: 10.1126/science.1209038.
12. Brodsky JL. Cleaning up: ER-associated degradation to the rescue. *Cell*. 2012;151:1163–1167. doi: 10.1016/j.cell.2012.11.012.
13. Claessen JH, Kundrat L, Ploegh HL. Protein quality control in the ER: balancing the ubiquitin checkbook. *Trends Cell Biol*. 2012;22:22–32. doi: 10.1016/j.tcb.2011.09.010.
14. Xu C, Bailly-Maitre B, Reed JC. Endoplasmic reticulum stress: cell life and death decisions. *J Clin Invest*. 2005;115:2656–2664. doi: 10.1172/JCI26373.
15. Sano R, Reed JC. ER stress-induced cell death mechanisms. *Biochim Biophys Acta*. 2013;1833:3460–3470. doi: 10.1016/j.bbamcr.2013.06.028.
16. Zhu C, Johansen FE, Prywes R. Interaction of ATF6 and serum response factor. *Mol Cell Biol*. 1997;17:4957–4966.
17. Haze K, Yoshida H, Yanagi H, Yura T, Mori K. Mammalian transcription factor ATF6 is synthesized as a transmembrane protein and activated by proteolysis in response to endoplasmic reticulum stress. *Mol Biol Cell*. 1999;10:3787–3799.
18. Glembotski CC. Roles for ATF6 and the sarco/endoplasmic reticulum protein quality control system in the heart. *J Mol Cell Cardiol*. 2014;71:11–15. doi: 10.1016/j.yjmcc.2013.09.018.
19. Lynch JM, Maillet M, Vanhoutte D, et al. A thrombospondin-dependent pathway for a protective ER stress response. *Cell*. 2012;149:1257–1268. doi: 10.1016/j.cell.2012.03.050.
20. Belmont PJ, Tadimalla A, Chen WJ, Martindale JJ, Thuerauf DJ, Marcinko M, Gude N, Sussman MA, Glembotski CC. Coordination of growth and endoplasmic reticulum stress signaling by regulator of calcineurin 1 (RCAN1), a novel ATF6-inducible gene. *J Biol Chem*. 2008;283:14012–14021. doi: 10.1074/jbc.M709776200.
21. Hampton RY, Gardner RG, Rine J. Role of 26S proteasome and HRD genes in the degradation of 3-hydroxy-3-methylglutaryl-CoA reductase, an integral endoplasmic reticulum membrane protein. *Mol Biol Cell*. 1996;7:2029–2044.
22. Bordallo J, Plemper RK, Finger A, Wolf DH. Der3p/Hrd1p is required for endoplasmic reticulum-associated degradation of misfolded lumenal and integral membrane proteins. *Mol Biol Cell*. 1998;9:209–222.
23. Gardner RG, Swarbrick GM, Bays NW, Cronin SR, Wilhovsky S, Seelig L, Kim C, Hampton RY. Endoplasmic reticulum degradation requires lumen to cytosol signaling. Transmembrane control of Hrd1p by Hrd3p. *J Cell Biol*. 2000;151:69–82.
24. Nadav E, Shmueli A, Barr H, Gonen H, Ciechanover A, Reiss Y. A novel mammalian endoplasmic reticulum ubiquitin ligase homologous to the yeast Hrd1. *Biochem Biophys Res Commun*. 2003;303:91–97.
25. Kikkert M, Doolman R, Dai M, Avner R, Hassink G, van Voorden S, Thanedar S, Roitelman J, Chau V, Wiertz E. Human HRD1 is an E3 ubiquitin ligase involved in degradation of proteins from the endoplasmic reticulum. *J Biol Chem*. 2004;279:3525–3534. doi: 10.1074/jbc.M307453200.
26. Omura T, Kaneko M, Okuma Y, Matsubara K, Nomura Y. Endoplasmic reticulum stress and Parkinson's disease: the role of HRD1 in averting apoptosis in neurodegenerative disease. *Oxid Med Cell Longev*. 2013;2013:239854. doi: 10.1155/2013/239854.
27. Hasegawa D, Fujii R, Yagishita N, et al. E3 ubiquitin ligase synoviolin is involved in liver fibrogenesis. *PLoS One*. 2010;5:e13590. doi: 10.1371/journal.pone.0013590.
28. Yamasaki S, Yagishita N, Nishioka K, Nakajima T. The roles of synoviolin in crosstalk between endoplasmic reticulum stress-induced apoptosis and p53 pathway. *Cell Cycle*. 2007;6:1319–1323.
29. Neutzner A, Neutzner M, Benischke AS, Ryu SW, Frank S, Youle RJ, Karbowski M. A systematic search for endoplasmic reticulum (ER) membrane-associated RING finger proteins identifies Nixin/ZNRF4 as a regulator of calnexin stability and ER homeostasis. *J Biol Chem*. 2011;286:8633–8643. doi: 10.1074/jbc.M110.197459.
30. Yu H, Kaung G, Kobayashi S, Kopito RR. Cytosolic degradation of T-cell receptor alpha chains by the proteasome. *J Biol Chem*. 1997;272:20800–20804.
31. Olden K, Pratt RM, Jaworski C, Yamada KM. Evidence for role of glycoprotein carbohydrates in membrane transport: specific inhibition by tunicamycin. *Proc Natl Acad Sci USA*. 1979;76:791–795.
32. Thastrup O, Cullen PJ, Drøbak BK, Hanley MR, Dawson AP. Thapsigargin, a tumor promoter, discharges intracellular Ca2+ stores by specific inhibition of the endoplasmic reticulum Ca2(+)-ATPase. *Proc Natl Acad Sci USA*. 1990;87:2466–2470.
33. Jämsä E, Simonen M, Makarow M. Selective retention of secretory proteins in the yeast endoplasmic reticulum by treatment of cells with a reducing agent. *Yeast*. 1994;10:355–370. doi: 10.1002/yea.320100308.
34. Ishikura S, Weissman AM, Bonifacino JS. Serine residues in the cytosolic tail of the T-cell antigen receptor alpha-chain mediate ubiquitination and endoplasmic reticulum-associated degradation of the unassembled protein. *J Biol Chem*. 2010;285:23916–23924. doi: 10.1074/jbc.M110.127936.
35. Boecker W, Bernecker OY, Wu JC, Zhu X, Sawa T, Grazette L, Rosenzweig A, del Monte F, Schmidt U, Hajjar RJ. Cardiac-specific gene expression facilitated by an enhanced myosin light chain promoter. *Mol Imaging*. 2004;3:69–75. doi: 10.1162/1535350041464847.
36. Müller OJ, Leuchs B, Pleger ST, Grimm D, Franz WM, Katus HA, Kleinschmidt JA. Improved cardiac gene transfer by transcriptional and transductional targeting of adeno-associated viral vectors. *Cardiovasc Res*. 2006;70:70–78. doi: 10.1016/j.cardiores.2005.12.017.
37. Völkers M, Konstandin MH, Doroudgar S, Toko H, Quijada P, Din S, Joyo A, Ornelas L, Samse K, Thuerauf DJ, Gude N, Glembotski CC, Sussman MA. Mechanistic target of rapamycin complex 2 protects the heart from ischemic damage. *Circulation*. 2013;128:2132–2144. doi: 10.1161/CIRCULATIONAHA.113.003638.
38. Völkers M, Toko H, Doroudgar S, Din S, Quijada P, Joyo AY, Ornelas L, Joyo E, Thuerauf DJ, Konstandin MH, Gude N, Glembotski CC, Sussman MA. Pathological hypertrophy amelioration by PRAS40-mediated inhibition of mTORC1. *Proc Natl Acad Sci USA*. 2013;110:12661–12666. doi: 10.1073/pnas.1301455110.
39. Minamino T, Kitakaze M. ER stress in cardiovascular disease. *J Mol Cell Cardiol*. 2010;48:1105–1110. doi: 10.1016/j.yjmcc.2009.10.026.
40. Christians ES, Mustafi SB, Benjamin IJ. Chaperones and cardiac misfolding protein diseases. *Curr Protein Pept Sci*. 2014;15:189–204.
41. Sandri M, Robbins J. Proteotoxicity: an underappreciated pathology in cardiac disease. *J Mol Cell Cardiol*. 2014;71:3–10. doi: 10.1016/j.yjmcc.2013.12.015.
42. Wang X, Robbins J. Proteasomal and lysosomal protein degradation and heart disease. *J Mol Cell Cardiol*. 2014;71:16–24. doi: 10.1016/j.yjmcc.2013.11.006.
43. Okada K, Minamino T, Tsukamoto Y, et al. Prolonged endoplasmic reticulum stress in hypertrophic and failing heart after aortic constriction: possible contribution of endoplasmic reticulum stress to cardiac myocyte apoptosis. *Circulation*. 2004;110:705–712. doi: 10.1161/01.CIR.0000137836.95625.D4.
44. Kim SK, Kim YK, Lee AS. Expression of the glucose-regulated proteins (GRP94 and GRP78) in differentiated and undifferentiated mouse embryonic cells and the use of the GRP78 promoter as an expression system in embryonic cells. *Differentiation*. 1990;42:153–159.
45. Barnes JA, Smoak IW. Immunolocalization and heart levels of GRP94 in the mouse during post-implantation development. *Anat Embryol (Berl)*. 1997;196:335–341.
46. Barnes JA, Smoak IW. Glucose-regulated protein 78 (GRP78) is elevated in embryonic mouse heart and induced following hypoglycemic stress. *Anat Embryol (Berl)*. 2000;202:67–74.
47. Mesaeli N, Nakamura K, Zvaritch E, Dickie P, Dziak E, Krause KH, Opas M, MacLennan DH, Michalak M. Calreticulin is essential for cardiac development. *J Cell Biol*. 1999;144:857–868.
48. Luo S, Mao C, Lee B, Lee AS. GRP78/BiP is required for cell proliferation and protecting the inner cell mass from apoptosis during early mouse embryonic development. *Mol Cell Biol*. 2006;26:5688–5697. doi: 10.1128/MCB.00779-06.
49. Yang Y, Liu B, Dai J, Srivastava PK, Zammit DJ, Lefrançois L, Li Z. Heat shock protein gp96 is a master chaperone for toll-like receptors and is important in the innate function of macrophages. *Immunity*. 2007;26:215–226. doi: 10.1016/j.immuni.2006.12.005.
50. Amano T, Yamasaki S, Yagishita N, et al. Synoviolin/Hrd1, an E3 ubiquitin ligase, as a novel pathogenic factor for arthropathy. *Genes Dev*. 2003;17:2436–2449. doi: 10.1101/gad.1096603.
51. Martindale JJ, Fernandez R, Thuerauf D, Whittaker R, Gude N, Sussman MA, Glembotski CC. Endoplasmic reticulum stress gene induction and

protection from ischemia/reperfusion injury in the hearts of transgenic mice with a tamoxifen-regulated form of ATF6. *Circ Res*. 2006;98:1186–1193. doi: 10.1161/01.RES.0000220643.65941.8d.
52. Thuerauf DJ, Marcinko M, Gude N, Rubio M, Sussman MA, Glembotski CC. Activation of the unfolded protein response in infarcted mouse heart and hypoxic cultured cardiac myocytes. *Circ Res*. 2006;99:275–282. doi: 10.1161/01.RES.0000233317.70421.03.
53. Wang ZV, Deng Y, Gao N, et al. Spliced X-box binding protein 1 couples the unfolded protein response to hexosamine biosynthetic pathway. *Cell*. 2014;156:1179–1192. doi: 10.1016/j.cell.2014.01.014.

Novelty and Significance

What Is Known?

- The endoplasmic reticulum (ER) is the location of the synthesis and folding of secreted and membrane proteins.
- A decrease in protein folding and accumulation of unfolded proteins in the ER may contribute to the pathology of several disease states.
- ER-associated degradation (ERAD) removes misfolded ER proteins and reduces and contributes to the adaptive rejuvenation of protein folding; however, the role of ERAD in cardiac myocytes and in heart disease has not been examined.

What New Information Does This Article Contribute?

- The ER-transmembrane protein, hydroxymethyl glutaryl-coenzyme A reductase degradation protein 1 (Hrd1), is expressed in the sarcoplasmic reticulum/ER of cardiac myocytes, where it ubiquitylates and targets misfolded proteins for removal, thus enhancing cell survival during stress.
- Increasing Hrd1 expression using an adeno-associated virus 9–based gene therapy approach preserved cardiac function and decreased cardiac hypertrophy in a model of pressure overload–induced cardiac pathology.
- Hrd1 plays a central role in ERAD and contributes to the ability of cardiac myocytes to adapt to pathological conditions that threaten myocyte viability by impairing ER protein folding.

The ER is the site of secreted and membrane protein synthesis and folding. In the diseased heart, impaired ER protein folding could contribute to pathology. The ER-transmembrane protein, Hrd1, is a ubiquitin ligase that has been shown in yeast to ubiquitylate misfolded, potentially toxic proteins, targeting them for degradation by ER-associated degradation, ERAD, which improves cell viability. However, neither Hrd1 nor ERAD has been studied in the heart. Accordingly, we examined the functions of Hrd1 and ERAD in cardiac myocytes and determined whether they play adaptive roles in the pathological heart. We found that cardiac myocytes express Hrd1 in the sarcoplasmic reticulum and that Hrd1 is required for ERAD. Knocking down Hrd1 decreased ERAD, increased misfolded ER protein accumulation, and decreased cardiac myocyte viability. When we knocked down Hrd1 in mouse hearts, in vivo, cardiac function was impaired in mice subjected to a surgery that causes pathological cardiac hypertrophy; in contrast, overexpression of Hrd1 preserved cardiac function. These findings suggest that overexpressing Hrd1 and improving ERAD in the heart have potential for the treatment of heart failure.

Supplemental Material

Detailed Methods:

Cultured Cardiac Myocytes: Neonatal rat ventricular myocyte cultures were prepared from 1 to 3 day-old Sprague-Dawley rat hearts using a neonatal cardiomyocyte isolation system (cat# LK003300 Worthington Biochemical Corp.). Myocytes were then purified on a discontinuous Percoll density gradient. Briefly, isolated cells were counted and collected by centrifugation at 250×g for 5 min in an Eppendorf 5810R using the swinging bucket rotor. Forty to 60 million cells were then resuspended in 2 ml of red (with phenol red) 1×ADS buffer (116mM NaCl, 18mM HEPES, 845μM $NaHPO_4$, 5.55mM Glucose, 5.37mM KCl, 831μM $MgSO_4$, 0.002% Phenol Red, pH 7.35±0.5). Stock Percoll was prepared by combining 9 parts of Percoll (cat# 17-0891-02, GE healthcare, Piscataway, NJ) with 1 part of clear (without phenol red) 10×ADS. The stock Percoll was used to make the Percoll for the top (density= 1.059 g/ml; 1 part Percoll stock added to 1.2 parts clear 1×ADS) and bottom (density= 1.082 g/ml; 1 part Percoll stock added to 0.54 parts red 1×ADS) layers. The gradient, consisting of 4 ml top Percoll and 3 ml bottom Percoll, was set in a 15 ml conical tube by pipetting the top Percoll first, and layering the bottom Percoll gently underneath, and the cells (in 2 ml red 1×ADS buffer) were layered on the top. Subsequently, the Percoll gradient was centrifuged at 1500×g for 30 min with no deceleration brake at room temperature. The isolated myocytes, which concentrated in the layer located between the lower red ADS layer and the middle clear ADS layer, were carefully collected and washed twice with 50 ml of 1×ADS, and were then resuspended in plating medium and counted. This procedure is also effective for purifying myocytes that have been isolated by trypsin digestion, as previously described[1]. Following Percoll purification, myocytes were plated at the desired density on plastic culture plates that had been pre-treated with 5 μg/ml fibronectin for one hour. Cultures were then maintained in Dulbecco's modified Eagle's medium (DMEM)/F12 (cat# 11330-32, Invitrogen, Carlsbad, CA), supplemented with 10% fetal calf serum and antibiotics (100 units/ml penicillin and 100 μg/ml streptomycin), and then switched to DMEM/F12 supplemented with 2% fetal calf serum for all of the experiments, except that shown in Online Figure V, which used DMEM/F12 in serum free medium.

^{3}H-Leucine Incorporation and Trichloroacetic Acid Precipitation of Protein: Neonatal rat ventricular myocytes were plated at 0.5 to 1.0×10^6 cells/well in a six-well plastic culture dish. Twenty-four hours after plating, cultures were infected with adenovirus in 1 ml of DMEM/F-12 supplemented with 2% fetal calf serum for overnight infections. The infection medium was then changed to DMEM/F-12 supplemented with 1% bovine serum albumin (serum-free medium) for forty-eight hours. The medium was then changed to serum-free medium with 10 μM phenylephrine, or without, for control. To this medium were added 1 μCi of ^{3}H-leucine (PerkinElmer NET460A001MC L-[3,4,5-^{3}H(N)]-Leucine, 100 to 150 Ci/mmol). Forty eight hours later the medium was removed, cultures were washed 3-times with 1 ml of DMEM/F-12, then 0.5 ml of 25% trichloroacetic acid were added and the cells were scraped and transferred to a 1.5-ml microcentrifuge tube. Fifty μl of a 10 mg/ml solution of bovine serum albumin were then added to induce protein precipitation. Samples were frozen overnight and after thawing, precipitates were collected by centrifugation at 4°C at ~20,000×g for 20 minutes. Supernatants were removed by careful manual aspiration using a pipette, and precipitated protein was dissolved in 200 μl of base buffer (1% Triton X-100, 1M NaOH)

at 37°C for two hours. Radioactivity in the solubilized material was then quantified by scintillation counting by placing 180 µl of the solubilized protein into 10 ml of Ecoscint scintillation fluid in glass scintillation vials. Each vial was counted for a minimum of 2 minutes. n = 6 cultures per treatment. Experiments were performed on at least 6 separate myocyte preparations.

Cultured Cardiac Myocyte Area: Neonatal rat ventricular myocytes (n = 3 cultures per treatment) were visualized by phase-contrast microscopy. The areas of each of 100-300 cells in images acquired from five different fields of each culture were determined using NIH Image J software. Experiments were performed on at least 3 separate myocyte preparations.

Hrd1 Antiserum Preparation and Characterization: A custom Hrd1 antiserum was generated in rabbits against a keyhole limpet hemocyanin-conjugated synthetic peptide, PEDGEPDAAELRRRRLQKLE, which is identical to residues 593-612 in the C-terminus of human Hrd1, and is conserved in residues 588-607 of mouse Hrd1, and in residues 584-603 of rat Hrd1. The cross-reactivity of the antibody against Hrd1 was shown by transfecting HeLa cells with an expression plasmid encoding either untagged, or FLAG-tagged mouse Hrd1, then demonstrating, by immunoblotting, that the Hrd1 antibody cross-reacts with endogenous and overexpressed Hrd1 at 68 kD, the predicted molecular mass or Hrd1. Moreover, when extracts from FLAG-Hrd1-transfected cells were examined, FLAG and Hrd1 cross-reactive material co-migrated on SDS gels, again, at about 68 kD. The specificity of the Hrd1 antiserum against endogenous and overexpressed Hrd1 was shown by blocking it with the peptide to which it was raised (see above), and then using immunoblotting to show that the 68 kD form of endogenous and overexpressed Hrd1 observed with the unblocked antiserum was not present when blocked antiserum was used.

siRNA Transfection into Cultured Cardiac Myocytes: Cultured cardiac myocytes were plated on 24 mm plates at 0.5 to 0.8 X 10^6 cells per well, then transfected with small interfering (si) RNA oligoribonucleotides targeted to rat Hrd1 (Life Sciences Technologies, Inc., Stealth siRNAs (set of 3) RSS324147, RSS324148, RSS324149), or control (Life Sciences Technologies, Inc.,12935-300). Each well was transfected with 10 pmoles of each siRNA using TransMessenger™ Transfection Reagent (Qiagen, Valencia, CA). After ~20h, in some cases, cells were treated with adenovirus for 24h, after which they were treated ± CHX (100mM) in 2% fetal calf serum containing media for varying times as shown in the figures.

Adenovirus (AdV): AdV-Hrd1- A recombinant Adv encoding full-length mouse Hrd1 (1-612) (Adv-Hrd1) was produced by first generating a PCR product that included the full-length mouse Hrd1 (NCBI RefSeq NM_028769) and cloning it into pcDNA3.1, from which the Hrd1 coding region was excised and cloned into the adenovirus shuttle vector, pAdTrack-CMV, which was then used to generate the desired Adv strain in 293 cells, as previously described[2]. A recombinant AdV encoding TCR-α-HA was produced by generating a PCR product from the plasmid template that was a generous gift from Dr. Ron Kopito, Stanford University, that included the full-length TCR-α and C-terminal HA epitope tag. All further cloning and AdV preparation was as described above for AdV-Hrd1.

Cell Extracts and Immunoprecipitation: Cells were extracted and subjected to immunoprecipitation and immunoblotting, as previously described[3].

Immunoblotting and Antibodies: The following antibodies were used at the following concentrations for immunoblotting: FLAG (Sigma-Aldrich F1804; 1:12,000), CHOP (Cell Signaling, D46F1, 1:1,000), Gapdh (RDI, TRK5G4; 1:150,000), HA-probe F-7 (Santa Cruz, SC-7392; 1:1,000), Hrd1 (see above; 1:20,000), and KDEL (ENZO Life Sciences; ADI-SPA-827; 1:8,000), which detects the C-terminal KDEL on Grp94 and Grp78.

Hrd1 Ubiquitylation Assay: To examine the ubiquitin ligase activity of Hrd1, HeLa cells were transfected with a plasmid encoding HA-tagged ubiquitin, and either a control plasmid, or a plasmid encoding mouse FLAG-mouse-Hrd1. Twenty-four hours later, extracts were either fractionated by SDS-PAGE, then examined by immunoblotting for Hrd1 and Gapdh, or they were subjected to FLAG immunoprecipitation, fractionated by SDS-PAGE, and then blotted for FLAG, in order to detect overexpressed FLAG-Hrd1. In some cases, FLAG-immunoprecipitates were blotted for HA in order to detect ubiquitin on immunoprecipitated FLAG-Hrd1. A HA-ubiquitin ladder demonstrates the ability of FLAG-Hrd1 to ubiquitin itself, which serves as an indicator of the ubiquitin ligase activity of Hrd1.

ERAD Assay: ER-associated degradation (ERAD) was determined using a C-terminally HA-tagged version of the model substrate, TCR-α, essentially as described [4]. Briefly, 24-48h after plating, neonatal rat ventricular myocytes, which in some cases had been treated with siRNA (e.g. si-Con or si-Hrd1) during plating, were infected with AdV-TCR-α-HA. In some cases, cultures were also infected with another AdV (e.g. AdV-Con or AdV-Hrd1). Twenty-four hours later, culture media was replaced with media containing 2% fetal calf serum and no AdV. Twenty-four hours later, cultures were treated with CHX (100mM) for the times shown in the figures, after which they were extracted, followed by SDS-PAGE, and then blotted for HA. The immunoblots were quantified by densitometry, and TCR-α-HA/Gapdh ratios were determined. In cases where the effects of Hrd1 overexpression or knockdown, or TM or TG treatment on ERAD were examined, the TCR-α-HA/Gapdh values, usually the average of n = 3 cultures/treatment, obtained with no CHX treatment were set to 1.0, and the relative levels of TCR-α-HA/Gapdh after 30, or 60 mins of CHX treatment were compared to it to obtain rates of TCR-α-HA degradation for a given treatment.

Quantitative Real Time PCR: Quantitative real time PCR (qRT-PCR) was carried out as previously described using primers for mouse Hrd1, ATF6, atrial natriuretic factor (ANF), B-type natriuretic peptide (BNP), Grp78, collagen 1A1, β-myosin heavy chain, β-actin and GAPDH, which have also been previously described[5].

Mouse Heart Extraction: Extracts from left ventricles were prepared by homogenization using a pestle (Wheaton; 358133) and a 1.5 ml microcentrifuge tube in RIPA buffer comprising NaCl 150 mM, Tris-HCl (pH 7.5) 20 mM, Triton-X 1%, Na deoxycholate 0.50%, sodium dodecyl sulfate 1%.

Adeno-associated Virus (AAV): To prepare AAV to knockdown Hrd1 in the heart, an shRNA targeted to mouse Hrd1 was prepared using the following oligonucleotides:

sense: GCTAGCGCTTCTGTGCAGCTGGTAGTTTTCAAGAGAAAATACCAGC

TCGACAGAAGCCTTTTGC

antisense: GCGAGCAAAAAGGCTTCTGTGCAGCTGGTATTTTCTCTTGAAAA
CTACCAGCTGCACAGAAGCG,

which were annealed and cloned into the NheI and XhoI sites in pTRUFU6. AAV9-sh-Con was prepared by cloning into pTRUFU6. An shRNA directed against a portion of firefly luciferase, which is predicted not to target any mouse transcripts, was generated as a control. The luciferase shRNA was prepared beginning with the following oligonucleotides:

sense: CTAGCGCTCAACAGTATGGGCATGTCTTCAAGAGAGAAATGCCC
ATACTGTTGAGCCTTTTTGC

antisense: GCGAGCAAAAAGGCTCAACAGTATGGGCATTTCTCTCTTGAA
GACATGCCCATACTGTTGAGCG,

which were annealed and cloned into the NheI and XhoI sites in pTRUFU6.

To prepare AAV to overexpress Hrd1 in the heart, the vector, pTRUF12, a gift from Dr. Roger Hajjar, was modified by removing the GFP downstream of the IRES, and adding restriction sites into the multiple cloning site to include Nhe1, Pme1, Xho1, and Mlu1. The CMV promoter was replaced with $CMV_{enh}MLC800$ promoter by standard cloning methods, to generate pTRUF-$CMV_{enh}MLC800$, which was used to generate AAV9-Con. The vector used to generate AAV9-Hrd1 was constructed by cloning the cDNA from pcDNA3.1-Hrd1 (mouse) into the Xho1 and HindIII sites in pTRUF- $CMV_{enh}MLC800$. To generate recombinant AAV9, HEK293T cells were transfected with pTRUF helper plasmid and the appropriate pTRUF-$CMV_{enh}MLC800$, or pTRUFU6 plasmids, and standard virus amplification, purification, and plaque assays were performed. For detailed protocol of AAV9 generation, see the Supporting Materials and Methods of [6]. To administer recombinant AAV, mice were anesthetized with 2% isofluorane and 100 ml of 37ºC heated Lactated Ringer's containing 10^{11} genome-containing units per mouse were injected via tail vein.

Immunocytofluorescence of Cultured Cardiac Myocytes: Neonatal rat ventricular myocytes, isolated as described above, were planed onto glass slides (Lab-Tec cat no. 177380 or 154461) that had been pretreated with fibronectin (25 μg/ml in serum free medium for 1h). Cells were plated in DMEM containing 10% fetal calf serum at a density of $2X10^6$ cells/chamber. Twenty-four hours later, cells were treated with the appropriate AdV, described above. Twenty-four hours later, the medium was changed to DMEM containing 10% fetal calf serum and, in some cases, cells were treated with TM (10 μg/ml) for 20h. Slides were then washed with PBS then fixed with 4% paraformaldehyde for 20 min, and then washed with PBS, permeabilized with 0.1% Triton X-100 in PBS for 10 min, washed with PBS and then blocked for 1h with 10% horse serum in PBS. After removal of the chamber and gasket, slides were incubated with the appropriate primary antibody diluted in 10% horse serum/PBS. The primary antibodies used were anti-Hrd1 at 1:200 or anti-KDEL at 1:200. Twenty-four hours later, slides were washed with PBS, then incubated with the appropriate secondary antibody, i.e. donkey anti-rabbit-FITC 1:300 and donkey-anti-mouse 1:300. Twenty-four hours later, TOPRO was added at 1:10,000 to stain nuclei, after which cells were mounted with Vectashield and images were obtained on a Zeiss 710 laser-scanning confocal microscope with a 63X objective.

Shown in each figure are small black and white images of each staining layer adjacent to the image of the merged layers.

Immunocytofluorescence of Mouse Heart Sections: Hearts were cleared by retroperfusion in situ with PBS at 70 mmHg, arrested in diastole with 60 mM KCl, fixed by perfusion for 15 min with 10% formalin (Sigma; HT501128), excised, fixed in formalin for 24 hours at room temperature, and embedded in paraffin. Paraffin-embedded hearts were sectioned and placed on slides, which were then deparaffinized, then rehydrated. Antigen retrieval was achieved by boiling the slides in 10 mM citrate pH 6.0 for 12 min, after which slides were washed several times with distilled water, and once with Tris/NaCl, or TN buffer (100 mM Tris, and 150 mM NaCl). Affinity-purified Hrd1 antiserum was diluted with TNB and added to slides which were incubated at 4 °C for approximately 12-16h. Samples were then washed with TN buffer and incubated with secondary antibodies at room temperature in the dark for 2 h. Images were obtained using a Leica TCS SP2 laser-scanning confocal microscope. Images were obtained with a 63X objective. Shown in each figure are small black and white images of each staining layer adjacent to the image of the merged layers.

TUNEL Assay: Terminal deoxynucleotidyl transferase dUTP nick-end labeling (TUNEL) staining was performed using the In Situ Cell Death Detection Kit, TMR red (Roche Applied Science). After deparaffinization, antigen retrieval was performed by boiling in 10 mM citrate in a microwave at 500 watts. Sections were incubated for 1 hour at 37°C with 0.5 μl of Enzyme diluted in 29.5 μl Dilution Buffer (Roche; 11966006001) and 25 μl Labeling Solution. Sections were then washed and incubated with Alexa fluor 488–conjugated wheat germ agglutinin (Life Technologies) for 1.5 hours, and with TOPRO for 15 min. TUNEL staining was quantified essentially as previously described[7] by examining ~3,000 nuclei from each of 5, or more randomly selected fields per heart. At least 4 hearts from each group were examined. Matched areas from the LV, IVS, and RV were sampled in each heart. Operators were blinded to treatments.

Trans-aortic Constriction: Trans-aortic constriction (TAC) was carried out essentially as described [8]. Briefly, adult male C57BL/6 **(Fig. 4)** or FVB **(Fig. 6)** mice were anesthetized with isofluorane, intubated, and a trans-sternal thoracotomy performed. A constriction of the aorta at the arch was performed by tying a 7.0 suture against a 27-gauge needle. The needle was removed leaving a calibrated stenosis of the aorta. Sham-operated mice were exposed to the same procedure, except that the aorta was not constricted. The chest was closed and the animals were allowed to recover.

Echocardiography: Echocardiography was carried out on anesthetized mice using a Visualsonics Vevo 770, or a Visualsonics Vevo 2100 high-resolution echocardiograph, as previously described [9].

Calcium Handling: Eight week-old FVB mice were treated with 10^{11} genome containing units of AAV9-Con or AAV9-Hrd1. Cardiac myocytes were isolated 3 weeks after AAV9 administration and used for Ca^{2+} handling experiments, as described [10].

Statistics: Cell culture experiments were performed at least 3 times with n = at least three cultures for each treatment. Values for data are mean ± standard error of the mean (SEM). Unless otherwise indicated, statistical treatments were by ANOVA followed by Newman-Keuls post hoc analysis.

Supplemental References:

1. Thuerauf DJ, Hoover H, Meller J, Hernandez J, Su L, Andrews C, Dillmann WH, McDonough PM, Glembotski CC. Sarco/endoplasmic reticulum calcium ATPase-2 expression is regulated by ATF6 during the endoplasmic reticulum stress response: intracellular signaling of calcium stress in a cardiac myocyte model system. *J Biol Chem.* 2001;276:48309-48317.

2. Thuerauf DJ, Marcinko M, Gude N, Rubio M, Sussman MA, Glembotski CC. Activation of the unfolded protein response in infarcted mouse heart and hypoxic cultured cardiac myocytes. *Circ Res.* 2006;99:275-282.

3. Glembotski CC, Thuerauf DJ, Huang C, Vekich JA, Gottlieb RA, Doroudgar S. Mesencephalic astrocyte-derived neurotrophic factor protects the heart from ischemic damage and is selectively secreted upon sarco/endoplasmic reticulum calcium depletion. *J Biol Chem.* 2012;287:25893-25904.

4. Yu H, Kaung G, Kobayashi S, Kopito RR. Cytosolic degradation of T-cell receptor alpha chains by the proteasome. *J Biol Chem.* 1997;272:20800-20804.

5. Martindale JJ, Fernandez R, Thuerauf D, Whittaker R, Gude N, Sussman MA, Glembotski CC. Endoplasmic reticulum stress gene induction and protection from ischemia/reperfusion injury in the hearts of transgenic mice with a tamoxifen-regulated form of ATF6. *Circ Res.* 2006;98:1186-1193.

6. Volkers M, Doroudgar S, Nguyen N, Konstandin MH, Quijada P, Din S, Ornelas L, Thuerauf DJ, Gude N, Friedrich K, Herzig S, Glembotski CC, Sussman MA. PRAS40 prevents development of diabetic cardiomyopathy and improves hepatic insulin sensitivity in obesity. *EMBO Mol Med.* 2014;6:57-65.

7. O'Connell TD, Swigart PM, Rodrigo MC, Ishizaka S, Joho S, Turnbull L, Tecott LH, Baker AJ, Foster E, Grossman W, Simpson PC. Alpha1-adrenergic receptors prevent a maladaptive cardiac response to pressure overload. *J Clin Invest.* 2006;116:1005-1015.

8. Rockman HA, Ross RS, Harris AN, Knowlton KU, Steinhelper ME, Field LJ, Ross J, Jr., Chien KR. Segregation of atrial-specific and inducible expression of an atrial natriuretic factor transgene in an in vivo murine model of cardiac hypertrophy. *Proc Natl Acad Sci U S A.* 1991;88:8277-8281.

9. Tsujita Y, Kato T, Sussman MA. Evaluation of left ventricular function in cardiomyopathic mice by tissue Doppler and color M-mode Doppler echocardiography. *Echocardiography.* 2005;22:245-253.

10. Respress JL, van Oort RJ, Li N, Rolim N, Dixit SS, deAlmeida A, Voigt N, Lawrence WS, Skapura DG, Skardal K, Wisloff U, Wieland T, Ai X, Pogwizd SM, Dobrev D, Wehrens XH. Role of RyR2 phosphorylation at S2814 during heart failure progression. *Circ Res.* 2012;110:1474-1483.

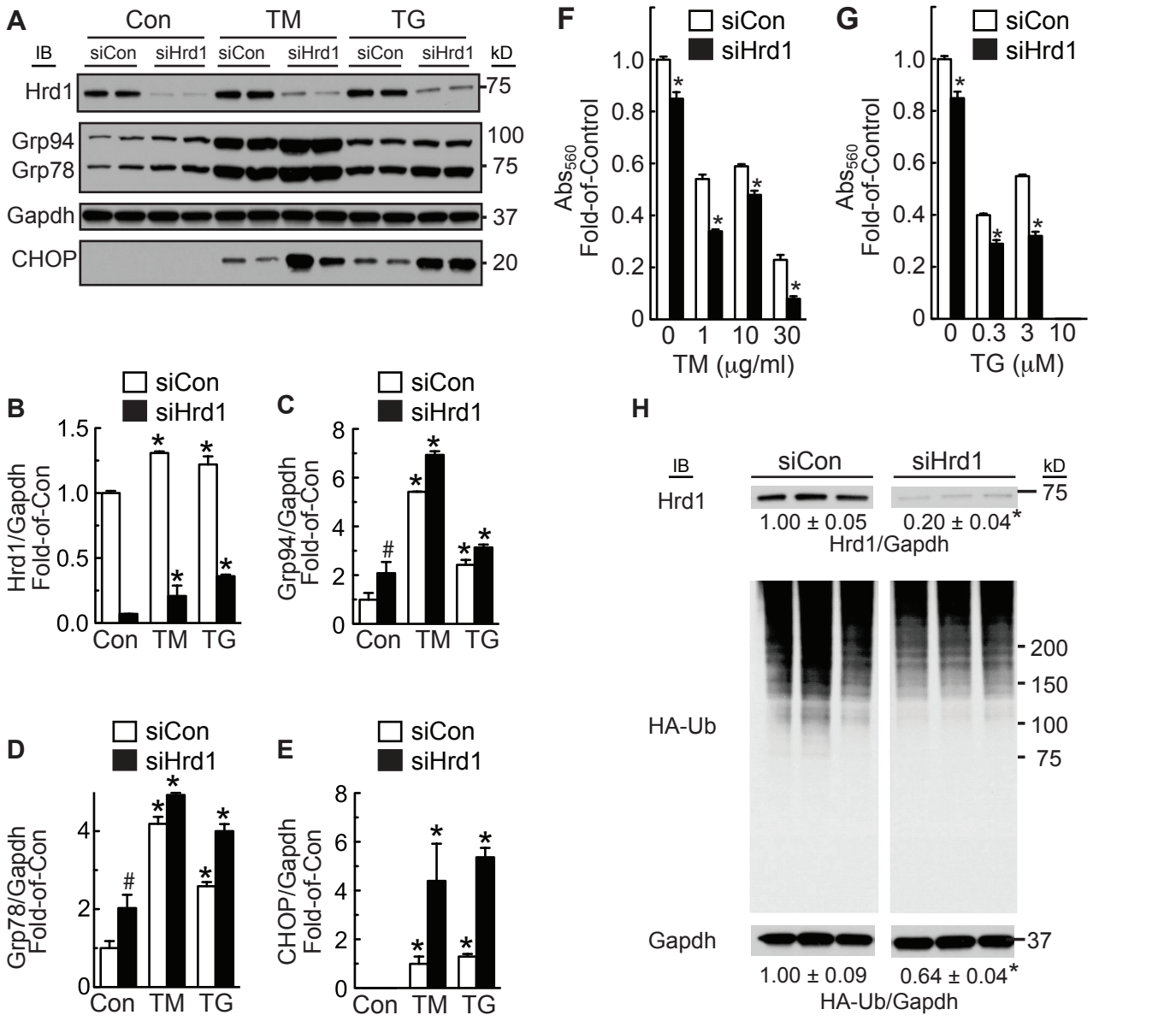

Online Figure I- Effects of Hrd1 Knockdown on Markers of ER Stress and Myocyte Viability
Cultured cardiac myocytes were treated with siCon or siHrd1 for 48h, then vehicle, TM (10 μg/ml) or TG (1 μM) for 72h. **A,** Hrd1, Grp94, Grp78, Gapdh, and CHOP were measured by immunoblotting. **B-E,** Densitometry of the blots shown in (a) normalized to vehicle-treated siCon, except for CHOP, which was normalized to TM-treated siCon. * = $p \leq 0.05$ different from Con; # = $p \leq 0.05$ different from Con/siCon by t-test. **F and G,** Cultured cardiac myocytes were treated as described in **A**, after which cell viability was determined by MTT assay. * = $p \leq 0.05$ different from siCon at the same dose and time of TM or TG treatment, as determined by t-test. **H,** Cultured cardiac myocytes were infected with AdV-HA-Ubiquitin and treated with either siCon or siHrd1. After 48h, extracts were analyzed for ubiquitylation by anti-HA immunoblotting. Densitometry was used to determine the relative levels of Hrd1 **(top)** and HA-Ub **(bottom)**. * = $p \leq 0.05$ different from siCon by t-test.

Online Figure I

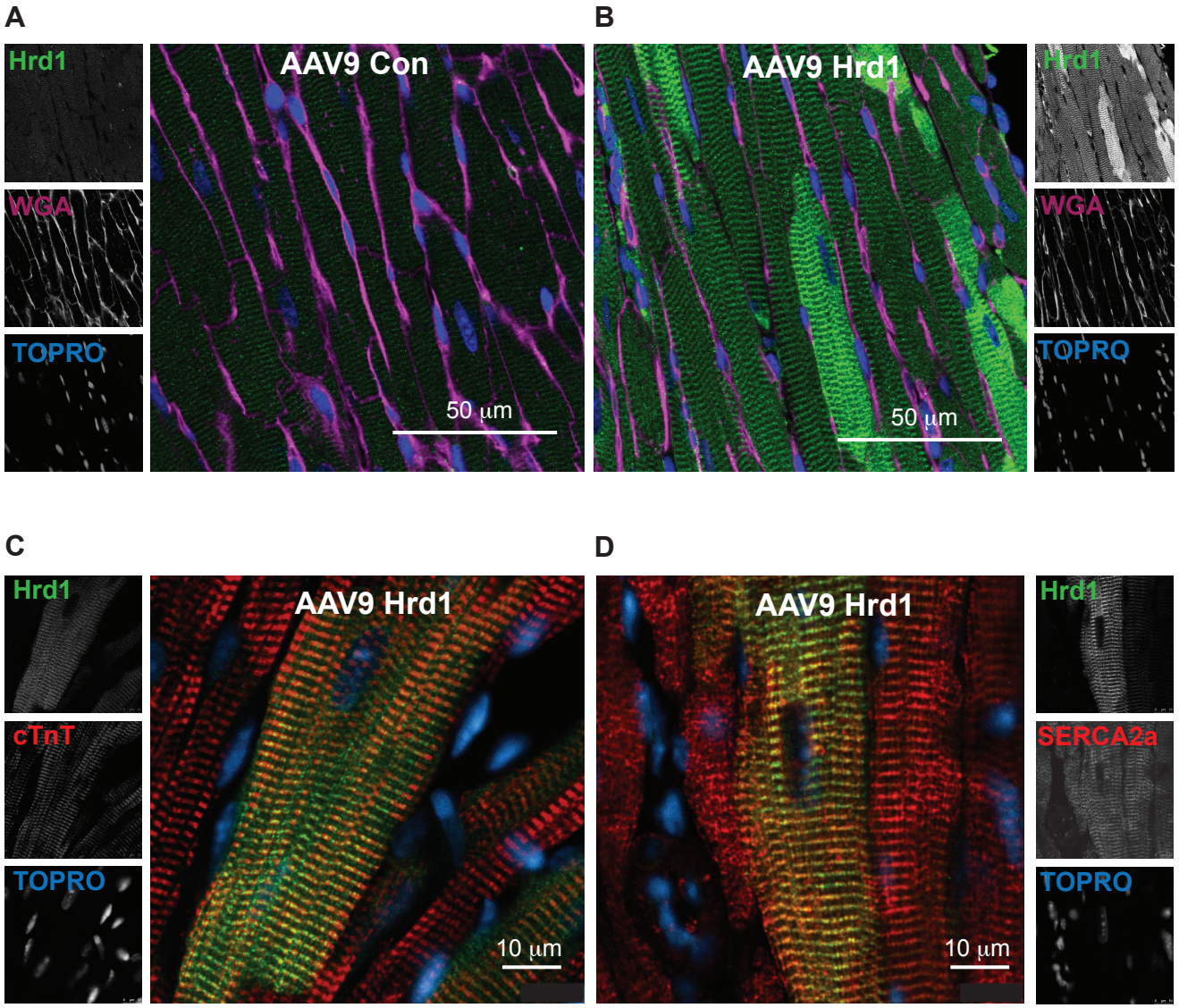

Online Figure II- Immunocytofluorescence Analaysis of Hrd1 Overexpression in Mouse Hearts
A and B, Confocal immunocytofluorescence microscopy analysis of mouse heart sections for Hrd1 (green), wheat germ agglutinin (WGA), to outline cells (magenta), and TOPRO for DNA (blue), in sections of hearts from mice treated for 6 weeks with AAV9-Con A, or AAV9-Hrd1 B. Bar = 50 μm.
C and D, Confocal immunocytofluorescence microscopy analysis of mouse heart sections for Hrd1 (green), cardiac troponin T (red) **C**, SERCA2a (red) **D**, and TOPRO for DNA (blue) in sections of hearts from mice treated for 6 weeks with AAV9-Hrd1. Bar = 10 μm.

Online Figure II

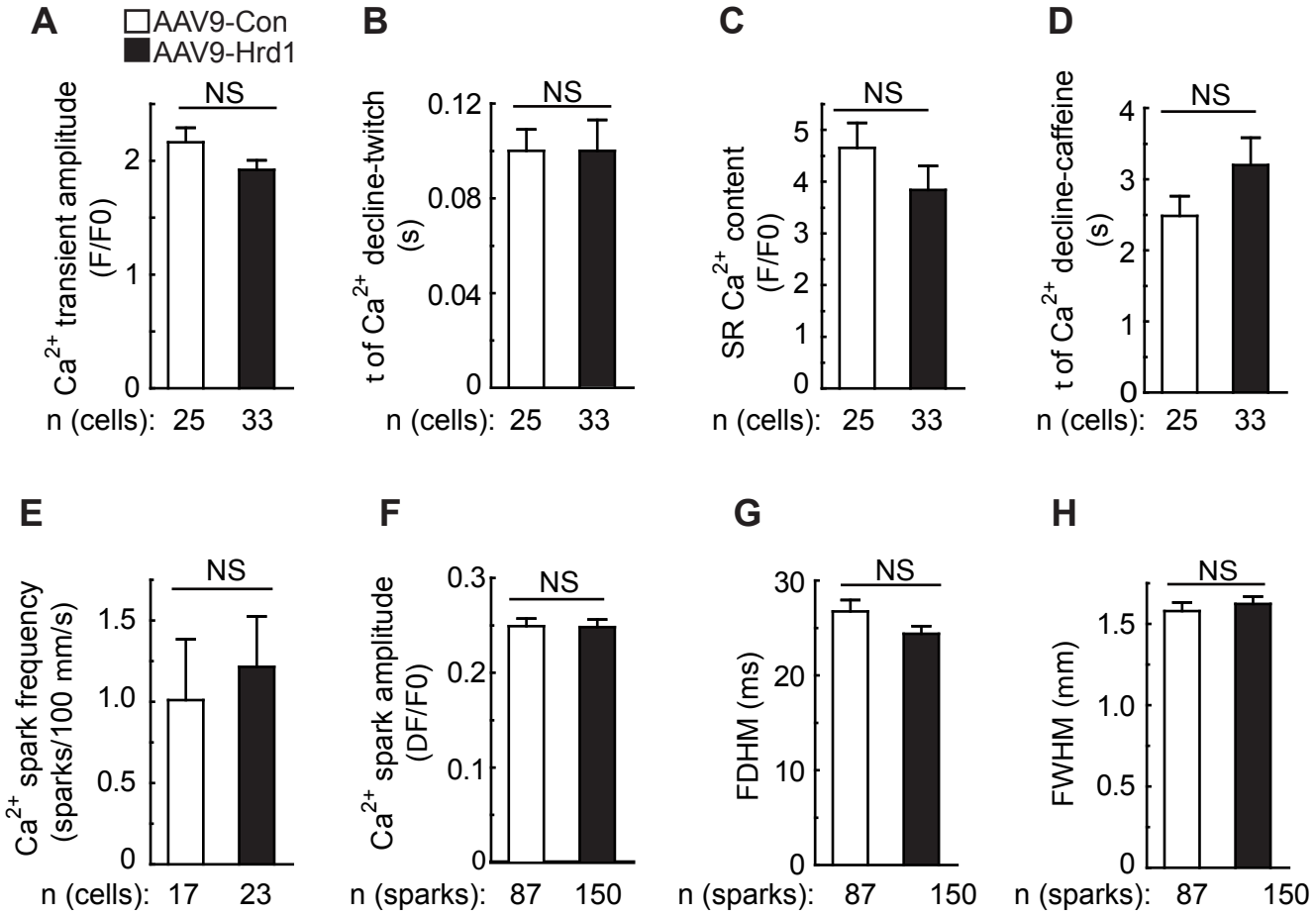

Online Figure III- Effect of Hrd1 overexpression on calcium handling in the heart
Cardiac myocytes were isolated from 11 week-old FVB mice 3 weeks after injection of $1x10^{11}$ genome containing units of AAV9-Con, or AAV9-Hrd1. **A,** Ca^{2+} transient amplitude; **B,** Half-life of Ca^{2+} decline (t); **C,** SR Ca^{2+} content after caffeine treatment; **D,** Half-life of Ca^{2+} decline (t) after caffeine treatment; **E,** Ca^{2+} spark frequency; **F,** Ca^{2+} spark amplitude; **G,** Ca^{2+} spark full duration at half-maximum (FDHM); **H,** Ca^{2+} spark full width at half-maximum (FWHM). NS = no significant differences.

Online Figure III

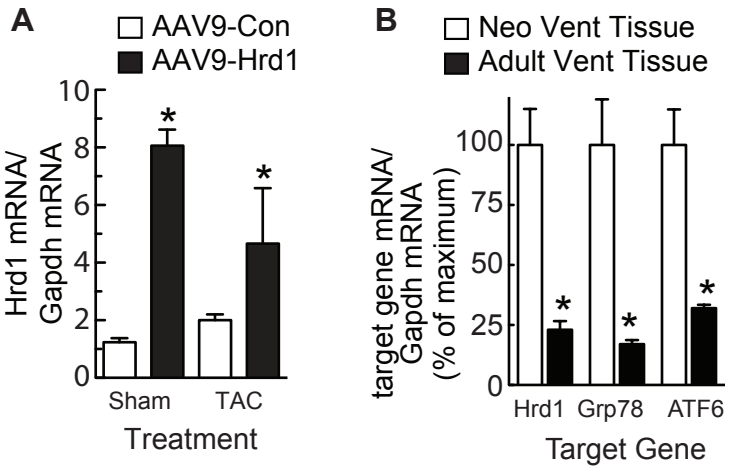

Online Figure IV- ER Stress Response Gene Levels in the Heart
A, The hearts from mice treated with either AAV9-Con or AAV9-Hrd1, then subjected to either sham or TAC surgery were extracted and analyzed for Hrd1 and Gapdh mRNA levels by qRT-PCR. n = 3 mice per treatment. * = $p \leq 0.05$ different from the AAV9-Con as determined by t-test. **B,** Hrd1, Grp78, ATF6 and Gapdh mRNA levels in neonatal (Neo) or adult rat ventricle (Vent) tissue extracts were measured by qRT-PCR. n = 5 samples of each. * = $p \leq 0.05$ different from neonatal ventricle tissue, as determined by t-test.

Online Figure IV

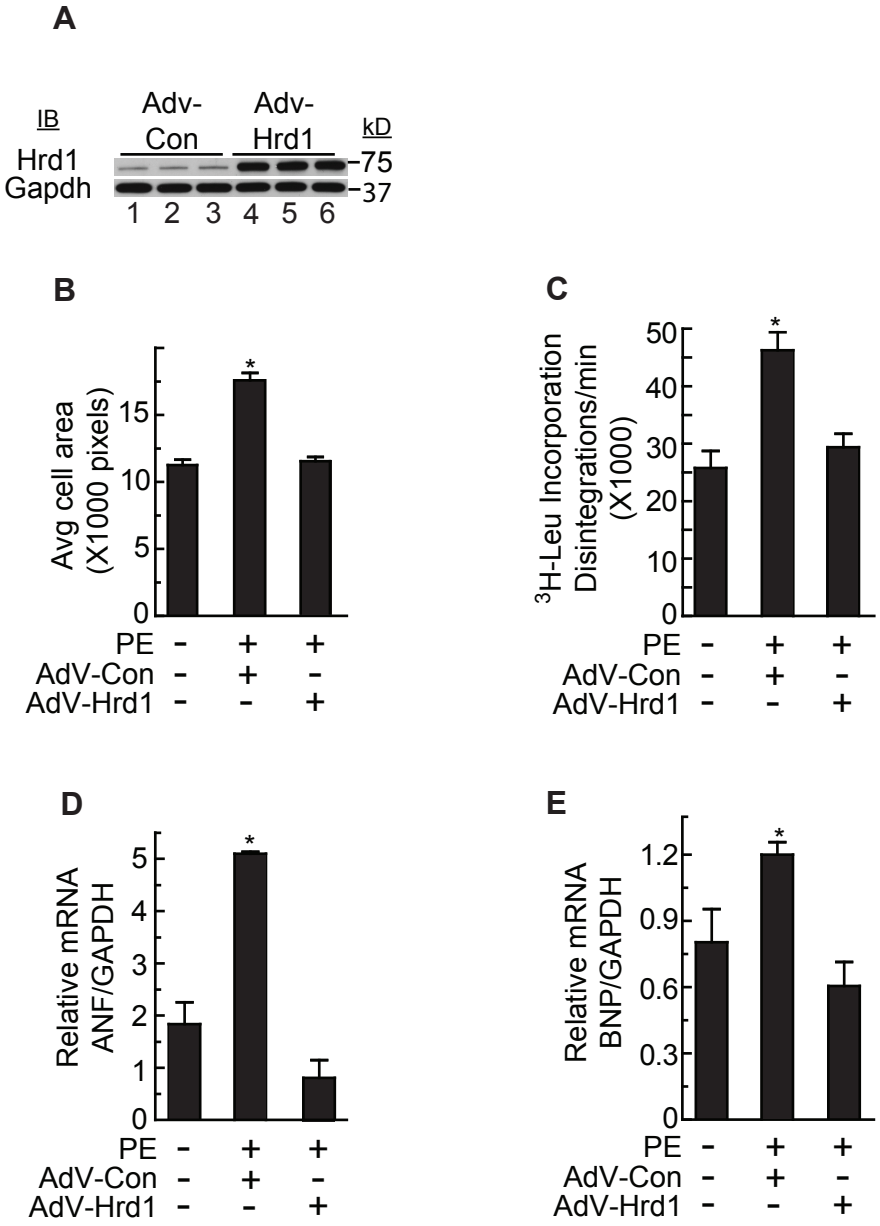

Online Figure V- Hrd1-dependent effects on cardiac myocyte hypertrophy

A, Representative immunoblot of protein extracts from Adv-Con and Adv-Hrd1 infected cultured cardiac myocytes. B-E, Myocytes were infected with AdV-Con or AdV-Hrd1 then treated with or without phenylephrine (PE), as shown. **B,** Cell size was determined by photomicroscopy, and morphometry, then expressed as mean ± SEM from from 3 independent experiments analyzing at least 300 cells per treatment per experiment. **C,** Incorporation of ^{3}H-leucine into TCA-precipitable protein in cardiac myocyte culture extracts. **D and E,** qRT-PCR examination of atrial natriuretic factor (ANF) **D,** and brain natriuretic peptide (BNP) **E,** mRNA levels in cardiac myocytes. *$p < 0.05$ different, as determined by t-test.

Online Figure V

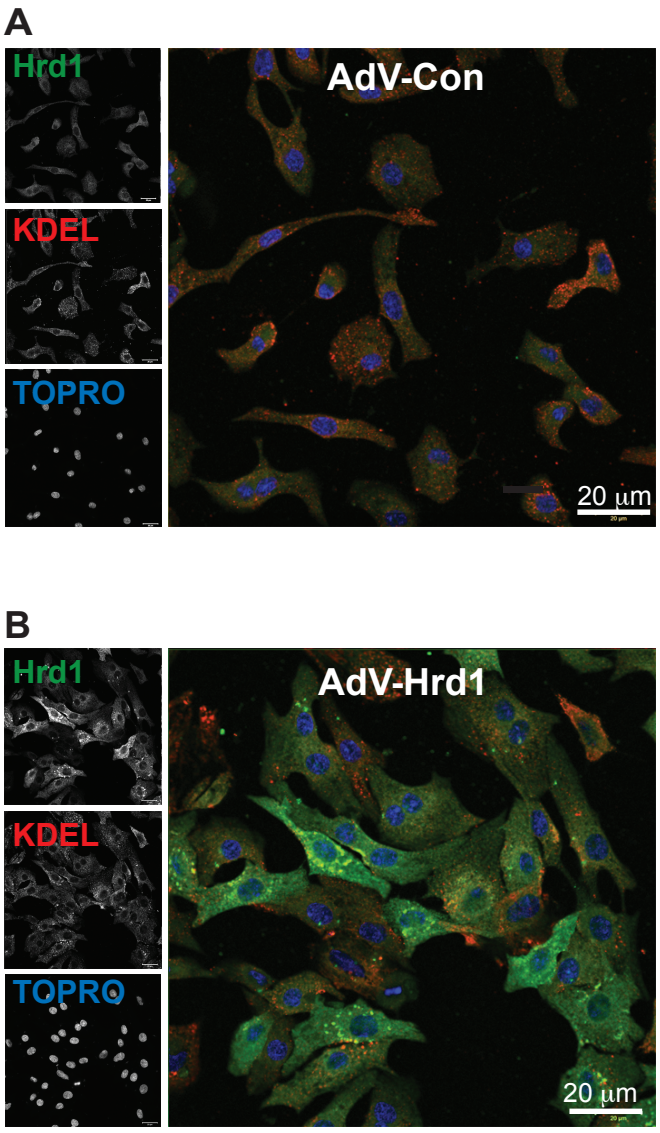

Online Figure VI- Immunocytofluorescence Characterization of Hrd1 Overexpression
A, Cultured cardiac myocytes were infected with AdV-Con or **B,** AdV-Hrd1 and 48h later, they were subjected to staining with TOPRO (nuclei; blue), anti-KDEL (ER; red), and anti-Hrd1 (green), followed by confocal microscopy. Bars = 20 μm

Online Figure VI

Online Table I: Echocardiographic parameters of mice treated with AAV9-sh-Con or AAV9-sh-Hrd1 and subjected to either sham or TAC surgery.

	AAV9-sh-Con sham (n = 8)	AAV9-sh-Hrd1 sham (n = 6)	AAV9-sh-Con TAC (n = 9)	AAV9-sh-Hrd1 TAC (n = 9)
FS (%)	24.0±0.76	26.2±1.50	16.5±1.23[1]	12.8±0.74[1,2]
EF (%)	48.3±1.28	51.7±2.36	34.7±2.38[1]	27.5±1.45[1,2]
LVEDV (μl)	69.6±1.86	70.0±1.73	78.5±3.65	105.0±36.08[1,2]
LVESV (μl)	37.1±1.78	35.0±2.53	53.9±4.74[1]	75.8±4.50[1,2]
LVIDD (mm)	4.03±0.04	4.04±0.05	4.25±0.09	4.73±0.10[1,2]
LVIDS (mm)	3.07±0.06	2.99±0.10	3.56±0.13[1]	4.12±0.11[1,2]
PWTD (mm)	0.85±0.03	0.87±0.02	1.04±0.04[1]	1.08±0.06[1]
PWTS (mm)	1.10±0.02	1.15±0.03	1.27±0.04[1]	1.26±0.06[1]
AWTD (mm)	0.81±0.03	0.86±0.04	1.13±0.05[1]	1.13±0.04[1]
AWTS (mm)	1.10±0.02	1.24±0.04	1.37±0.07[1]	1.39±0.05[1]
LV mass (mg)	95.0±3.50	106.4±4.36	152.8±10.50[1]	183.8±14.42[1,2]
HR (bpm)	503±16	538±10	458±16	448±17

FS = fractional shortening
EF = ejection fraction
LVEDV = left ventricular end diastolic volume
LVESV = left ventricular end systolic volume
LVIDD = left ventricular inner diameter in diastole
LVIDS = left ventricular inner diameter in systole
PWTD = left ventricular posterior wall thickness in diastole
PWTS = left ventricular posterior wall thickness in systole
AWTD = left ventricular anterior wall thickness in diastole
AWTS = left ventricular anterior wall thickness in systole
LV mass = left ventricular mass
HR = heart rate in beats per minute

Statistical analyses used a one way ANOVA with a Newman-Keuls post-hoc analysis.

[1] = $p \leq 0.05$ different from AAV9-sh-Con sham
[2] = $p \leq 0.05$ different from AAV9-sh-Con TAC

Online Table II: Echocardiographic parameters of mice treated with AAV9-Con or AAV9-Hrd1 and subjected to either sham or TAC surgery.

	AAV9-Con sham (n = 5)	AAV9-Hrd1 sham (n = 4)	AAV9-Con TAC (n = 11)	AAV9-Hrd1 TAC (n = 10)
FS (%)	43.2±3.20	40.1±2.55	30.1±1.70[1]	40.0±3.45
EF (%)	75.0±3.43	71.2±3.04	57.4±266[1]	70.1±4.30
LVEDV (μl)	39.80±3.40	52.7±6.23	70.23±5.15[1]	52.93±3.85
LVESV (μl)	10.03±1.85	17.33±2.75	30.82±3.96[1]	16.41±375
LVIDD (mm)	3.15±0.11	3.74±0.23	3.98±0.12[1]	3.54±0.11
LVIDS (mm)	1.79±0.13	2.24±0.15	2.80±0.14[1]	2.13±0.17
PWTD (mm)	1.30±0.13	0.89±0.04	1.08±0.07[1]	1.20±0.06
PWTS (mm)	1.74±0.05	1.46±0.07	1.39±0.06	1.66±0.08
AWTD (mm)	1.07±0.04	0.98±0.06	1.07±0.04	1.11±0.03
AWTS (mm)	1.40±0.07	1.39±0.06	1.54±0.04	1.57±0.03
LV mass (mg)	116.9±12.69	105.0±12.52	175.5±8.57[1]	159.5±5.75
HR (bpm)	417±21.6	427±15.3	497±27.8	443±27.3

FS = fractional shortening
EF = ejection fraction
LVEDV = left ventricular end diastolic volume
LVESV = left ventricular end systolic volume
LVIDD = left ventricular inner diameter in diastole
LVIDS = left ventricular inner diameter in systole
PWTD = left ventricular posterior wall thickness in diastole
PWTS = left ventricular posterior wall thickness in systole
AWTD = left ventricular anterior wall thickness in diastole
AWTS = left ventricular anterior wall thickness in systole
LV mass = left ventricular mass
HR = heart rate in beats per minute

Statistical analyses used a one way ANOVA with a Newman-Keuls post-hoc analysis.

[1] = $p \leq 0.05$ different from AAV9-Con sham
[2] = $p \leq 0.05$ different from AAV9-Con TAC

Circulation Research
JOURNAL OF THE AMERICAN HEART ASSOCIATION

Hrd1 and ER-Associated Protein Degradation, ERAD, Are Critical Elements of the Adaptive ER Stress Response in Cardiac Myocytes

Shirin Doroudgar, Mirko Völkers, Donna J. Thuerauf, Mohsin Khan, Sadia Mohsin, Jonathan L. Respress, Wei Wang, Natalie Gude, Oliver J. Müller, Xander H.T. Wehrens, Mark A. Sussman and Christopher C. Glembotski

Circ Res. 2015;117:536-546; originally published online July 2, 2015;
doi: 10.1161/CIRCRESAHA.115.306993
Circulation Research is published by the American Heart Association, 7272 Greenville Avenue, Dallas, TX 75231

Print ISSN: 0009-7330. Online ISSN: 1524-4571